Geological Carbon Sequestration Storage Resource Estimates for the Ordovician St. Peter Sandstone, Illinois and Michigan Basins, USA

TOPICAL REPORT

December 8, 2009 through June 30, 2014

David A. Barnes[1] and Kevin M Ellett[2]
[1]Department of Geosciences
Western Michigan University
1903 W Michigan Ave
Kalamazoo, MI 49008-5241 USA
[2]Indiana Geological Survey
Indiana University
611 N. Walnut Grove Ave.
Bloomington, IN 47405 USA

Report issued: July 11, 2014

Report Number: DOE/FE0002068-6
U.S. DOE Cooperative Agreement Number: DE-FE0002068
An Evaluation of the Carbon Sequestration Potential of the Cambro-Ordovician Strata of the Illinois and Michigan Basins

Principal Investigator: Dr. Hannes Leetaru
Business Contact: Illinois State Geological Survey
615 E. Peabody Drive
Champaign, IL 61820-7406

ABSTRACT

The Cambro-Ordovician strata of the Midwest of the United States is a primary target for potential geological storage of CO_2 in deep saline formations. The objective of this project is to develop a comprehensive evaluation of the Cambro-Ordovician strata in the Illinois and Michigan Basins above the basal Mount Simon Sandstone since the Mount Simon is the subject of other investigations including a demonstration-scale injection at the Illinois Basin Decatur Project. The primary reservoir targets investigated in this study are the middle Ordovician St Peter Sandstone and the late Cambrian to early Ordovician Knox Group carbonates. The topic of this report is a regional-scale evaluation of the geologic storage resource potential of the St Peter Sandstone in both the Illinois and Michigan Basins.

Multiple deterministic-based approaches were used in conjunction with the probabilistic-based storage efficiency factors published in the DOE methodology to estimate the carbon storage resource of the formation. Extensive data sets of core analyses and wireline logs were compiled to develop the necessary inputs for volumetric calculations. Results demonstrate how the range in uncertainty of storage resource estimates varies as a function of data availability and quality, and the underlying assumptions used in the different approaches. In the simplest approach, storage resource estimates were calculated from mapping the gross thickness of the formation and applying a single estimate of the effective mean porosity of the formation. Results from this approach led to storage resource estimates ranging from 3.3 to 35.1 Gt in the Michigan Basin, and 1.0 to 11.0 Gt in the Illinois Basin at the P10 and P90 probability level, respectively. The second approach involved consideration of the diagenetic history of the formation throughout the two basins and used depth-dependent functions of porosity to derive a more realistic spatially variable model of porosity rather than applying a single estimate of porosity throughout the entire potential reservoir domains. The second approach resulted in storage resource estimates of 3.0 to 31.6 Gt in the Michigan Basin, and 0.6 to 6.1 Gt in the Illinois Basin. The third approach attempted to account for the local-scale variability in reservoir quality as a function of both porosity and permeability by using core and log analyses to calculate explicitly the net effective porosity at multiple well locations, and interpolate those results throughout the two basins. This approach resulted in storage resource estimates of 10.7 to 34.7 Gt in the Michigan Basin, and 11.2 to 36.4 Gt in the Illinois Basin. A final approach used advanced reservoir characterization as the most sophisticated means to estimating storage resource by defining reservoir properties for multiple facies within the St Peter formation. This approach was limited to the Michigan Basin since the Illinois Basin data set did not have the requisite level of data quality and sampling density to support such an analysis. Results from this approach led to storage resource estimates of 15.4 Gt to 50.1 Gt for the Michigan Basin. The observed variability in results from the four different approaches is evaluated in the context of data and methodological constraints, leading to the conclusion that the storage resource estimates from the first two approaches may be conservative, whereas the net porosity based approaches may over-estimate the resource.

OBJECTIVES

The objective of this study is the determination of geological carbon sequestration (GCS) storage resource estimates (SRE) for the prospective St. Peter Sandstone reservoir interval in the Illinois and Michigan basins of Illinois, Kentucky, Indiana, and Michigan. In these intracratonic, structural basins large areas of the land surface are underlain by the St. Peter Sandstone at depths in the subsurface below minimum formation pressures and temperatures sufficient to retain injected carbon dioxide (CO_2) in a dense, liquid-like supercritical phase (greater than ~800 m below the surface). SRE in the St. Peter Sandstone and other Cambro-Ordovician formations in this area are important since in many areas of the upper Midwest the world class, Cambrian Mount Simon Sandstone GCS reservoir is either absent or occurs at depths in the subsurface where burial induced lithification, physical compaction and/or cementation have eliminated pore space and GCS potential (Figure 4; DOE-NETL, 2012).

An important aspect of this study is the compilation of subsurface geological data suitable for use in SRE analysis and the assessment of the quality and spatial distribution of these data in order to infer appropriate confidence levels for SRE. U.S. DOE methodology for SRE on a national and regional scale (Goodman and others, 2011) provides a standardized approach for this analysis on the basis of a wide range of data quality and quantity, and this methodology is used in this study. As a result of active, deep (> 1500 to 2000 m), petroleum exploration and production drilling for Ordovician sandstone targets (now confidently identified as the St. Peter Sandstone) in the Michigan basin, substantial modern subsurface geological data is available throughout the basin including conventional core and core analysis data from nearly 100 wells and modern, high quality petrophysical wire-line log data from complete penetrations of the formation in over 250 wells. Although recent drilling and coring of the St Peter Sandstone in the Illinois Basin is limited to a few wells associated with GCS research, the compilation and analysis of prior records housed across the three-state region provided a data set of core analyses and wire-line log data from more than 70 wells for this study.

INTRODUCTION

Regional Geological Background

The Middle Ordovician (Whiterockian to Mohawkian; Barnes and others, 1996) age St. Peter Sandstone is a widespread, lithologically distinct, typically pure quartz arenite lithostratigraphic unit found throughout the upper Midwest, USA. The geological occurrence of the St. Peter ranges from surface outcrop to deep burial settings in the cratonic interior Michigan and Illinois basins at depths in excess of 3.5 km (Dapples, 1955; Willman and others, 1975; Catacosinos and Daniels, 1991; this paper). The St. Peter Sandstone was initially defined (Owen, 1847) as “ortho” quartzite sandstone exposed in Minneapolis and St. Paul, Minnesota, along the "St. Peter River", which is now called Minnesota River. The type section is in a bluff where the Minnesota joins the Mississippi River at Fort Snelling in Minneapolis.

The St. Peter and transitional/correlative, carbonate-dominated facies occur throughout much of the central US, including at least some portions of the states of Indiana, Ohio, Iowa, Kansas, Kentucky, Michigan, Minnesota, Missouri, and Nebraska (Dapples, 1955; Figure 1). Similar lithostratigraphic units of the Simpson Group are also recognized as far south as Oklahoma and Arkansas (Dapples, 1955). In the upper Midwest, the St. Peter ranges in thickness from a widespread stratigraphic pinch out (typically on structural arch settings, e.g. Kankakee, Findley-Algonquin, Wisconsin, and Cincinnati arches) to in excess of 330 m (1200 ft) in the Michigan basin (Figure 2). In structurally positive arch areas of the upper Midwest the St. Peter typically overlies a deep erosion surface or is absent (Figure 3) above the inter-regional, base Tippecanoe (Knox) unconformity, which was cut into various older strata (Sloss, 1963; USGS, 1992). In some areas of Wisconsin, southern Lower Michigan (Mai and Dott, 1985; this work), Indiana (Droste and others, 1982) and elsewhere, closely spaced stratigraphic sections of the St. Peter infill erosional relief on the unconformity surface in thickness of as much as 70-100 m within a few kilometers or less of stratigraphic sections where the St. Peter is thin or absent. In contrast, the contact with Lower-Middle Ordovician strata of the Knox and equivalent strata including the Prairie du Chien Group is considered conformable in the central portions of the Michigan and Illinois basins (see discussion in Catacosinos and Daniels, 1991; Barnes, and others, 1996). On the basis of biostratigraphic studies (summarized in Barnes, and others, 1996), within the central Illinois and Michigan basins the St. Peter sandstone is older (Whiterockian), whereas it appears to be younger (Mohawkian) in the Upper Mississippi Valley type section area and other arch areas of the upper Midwest (Figure 4). These age

relations suggest that deposition of the St. Peter was time transgressive from the central Michigan and Illinois basins outwards to arch areas such as southeastern Minnesota.

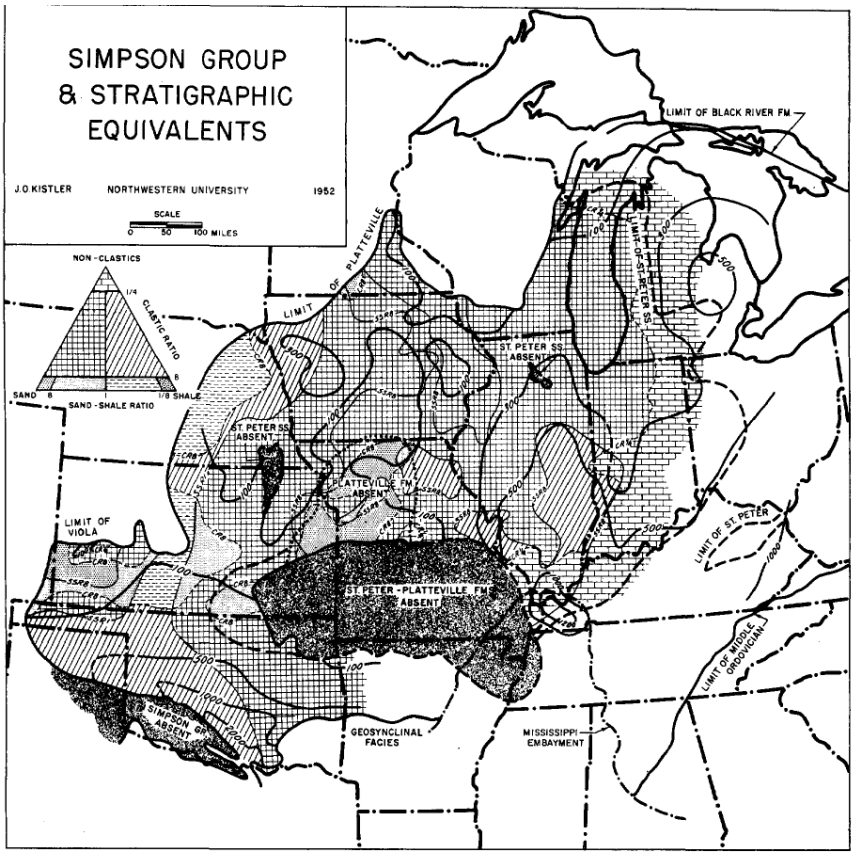

Figure 1. Map showing the isopach and lithofacies of the St. Peter Sandstone and Simpson Group in the central USA. Subsequent work suggests a somewhat different distribution of the St. Peter, especially in the Michigan and Illinois basins (see Figure 2). Reproduced from Dapples, 1955.

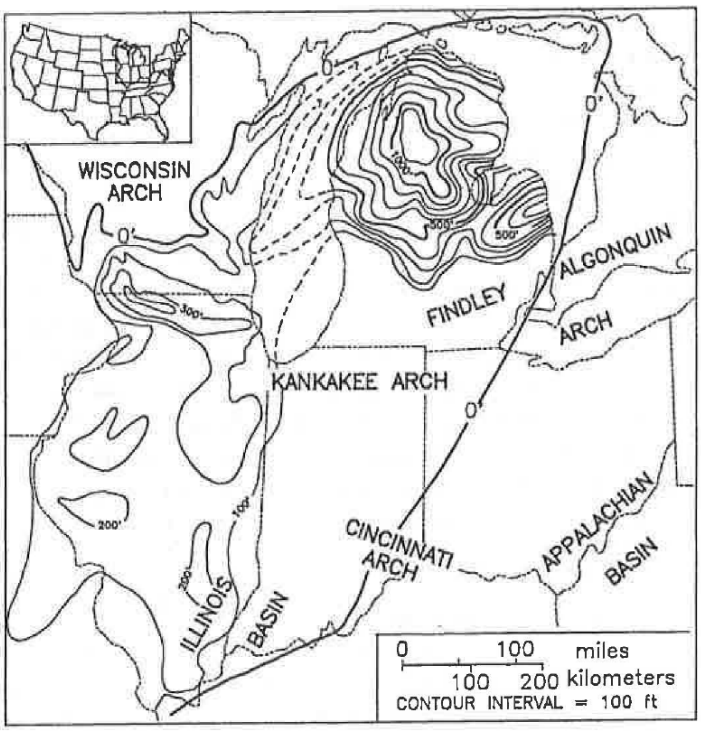

Figure 2. Generalized, regional St. Peter Sandstone isopach map in the Midwest Basins and Arches geologic province (reproduced from Barnes, and others, 1996). Lithofacies transitions in the St. Peter to carbonate-prone strata towards the east and south result in uncertainty in the placement of the zero isopach line. In other positive, cratonic arch areas where the St. Peter Sandstone isopach thins, sandstone lithofacies are irregularly distributed with depositional outliers present in isolated areas above the base Tippecanoe unconformity surface.

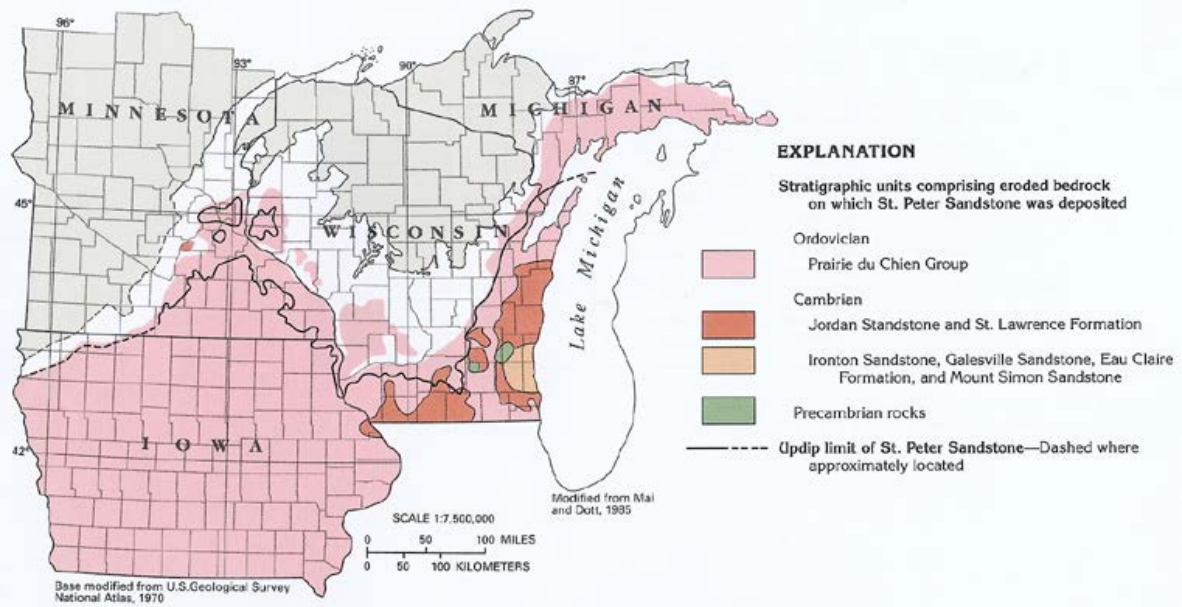

Figure 3. Stratigraphic units underlying the St. Peter Sandstone and the base-Tippecanoe unconformity surface in Minnesota, Iowa, Wisconsin and Northern MI (Olcott, 1992)

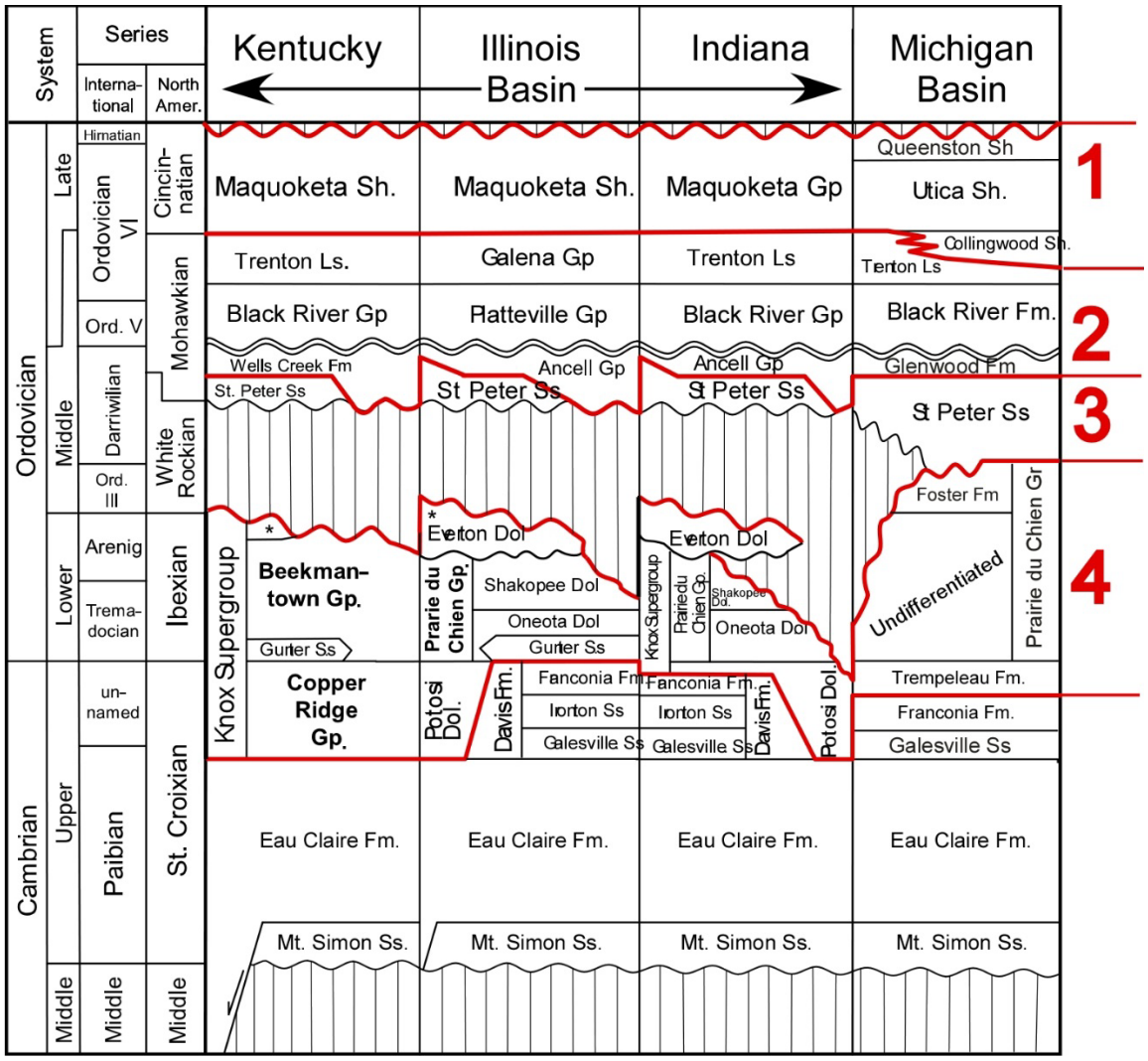

Figure 4. Lithostratigraphic correlation of Cambro-Ordovician strata in the Illinois and Michigan basins. 1. Primary confining layers of predominantly mudrock, Maquoketa, Utica, and Collingwood formations; 2. Secondary confining layers of predominantly non-reservoir carbonate and minor mixed, fine-grained clastics, Trenton, Black River, Galena, Platteville, and Glenwood-Wells Creek formations; 3. The subject of this study, prospective GCS reservoir, the St. Peter Sandstone; 4. Mixed reservoir and confining layers of dolomitic carbonate and minor, but significant, clastics; Knox Supergroup and Prairie du Chien Group and Trempeleau Formation.

The reservoir[1] potential of the St. Peter Sandstone is well established on the basis of historic potable water production in the upper Midwest (USGS, 1992; USGS, 1995) and successful natural gas storage operations in Illinois (Udegbunam, and others, 2001). More recently, active deep exploration well drilling,has resulted in commercial natural gas, natural gas liquids and minor petroleum being produced from the St. Peter Sandstone (also known as the "PDC" Sands by the Michigan Department of Oil, Gas, and Minerals) in 75 fields from over 250 wells (~110 currently producing) in the Michigan basin. This production is noteworthy because producing intervals occur at depths in excess of between 2000 to 3000 m in generally strongly indurated and cemented sandstone lithofacies. These lithologic properties are in marked contrast to shallow aquifers in the upper Midwest, which typically produce from friable, fine- to medium-grained well sorted and rounded quartz-arenite at depths typically less than a few hundred meters (USGS, 1992; USGS, 1995). The St. Peter Sandstone has been studied and exploited for natural gas storage in Illinois (Buschbach and Bond, 1974) at depths of less than 1 km but at depths below the occurrence of ground water of less than 10,000 ppm TDS (Figure5). The St. Peter in these fields possesses excellent reservoir quality with average porosity of 14%-16%ϕ and average permeability of 150 - 400 md. Petrologic study of the St Peter Sandstone in the Hillboro storage field of Montgomery Co., IL at burial depths of ~1000 m suggests incipient to significant lithification through compaction and diagenetic cementation of primary intergranular porosity (Udegbunam, and others, 2001), although reservoir quality is very good in these relatively shallowly buried sandstones with of 5%ϕ to over 25%ϕ and permeability from 10 md to over 1000 md.

[1] Porous and permeable strata capable of producing or accepting, through injection, commercial quantities of fluids, e.g. water, gas or petroleum.

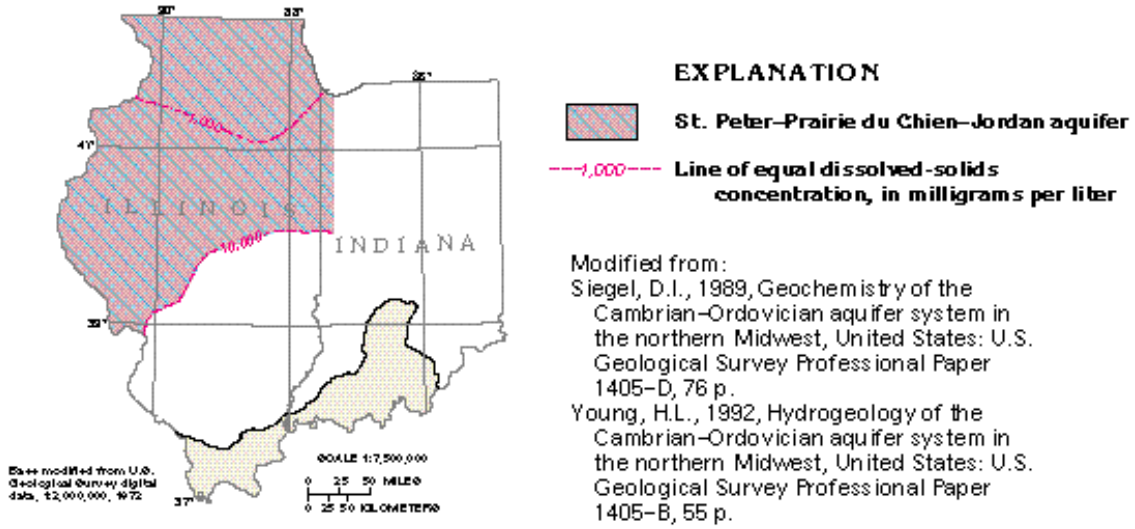

Figure 5. Ordovician aquifers including the St. Peter Sandstone in northern Illinois and Indiana (USGS, 1995)

The St. Peter Sandstone in the Michigan and Illinois Basins

Definition and Subsurface Expression of the St. Peter Sandstone in the Michigan basin

The St. Peter Sandstone is present throughout much of the subsurface of central and northern Lower Michigan from a stratigraphic pinch-out in the south to over 350 m in the basin center and at depths between 900 m and 3500 m below the surface (Figures 6 and 7). The St. Peter is identified in hundreds of well penetrations in the basin but only modern high quality (density-neutron porosity, +/- photo electric) logs with complete penetration of the formation (to at least the subjacent Prairie du Chien Group strata) were used in these maps and the following analysis.

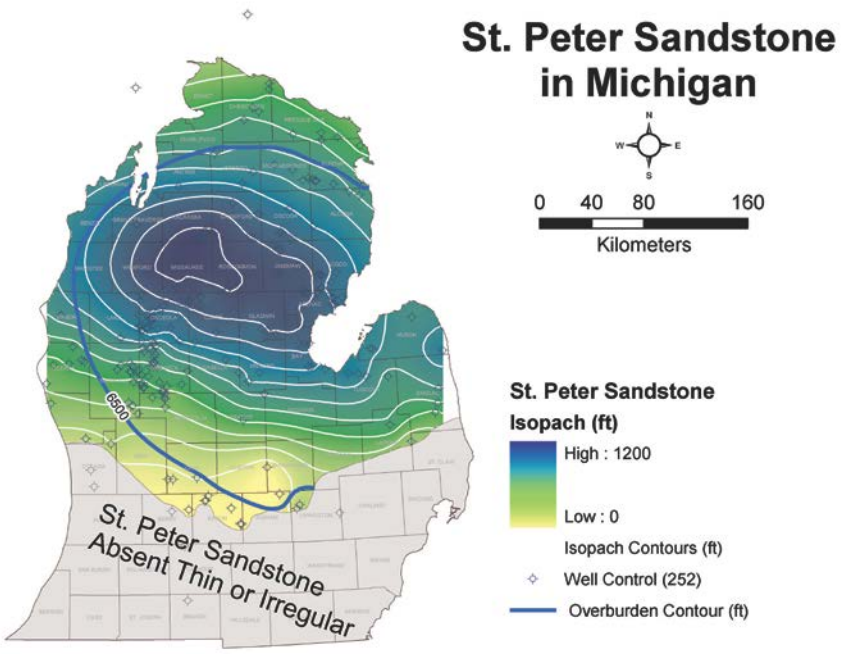

Figure 6. Isopach map of the St. Peter Sandstone in central and northern Lower Michigan. Contours are 100 ft. and the 6500 ft overburden contour included for reference. Note that isopachs are shifted to the north and west of the center of composite Paleozoic subsidence in the basin. This relationship and facies patterns (see text) are interpreted to indicate a predominantly (modern) north-westerly provenance for coarse-grained, quartzose of clastics, in the ancestral Wisconsin Highlands, for the St. Peter in Michigan and a south-easterly paleo-dip direction.

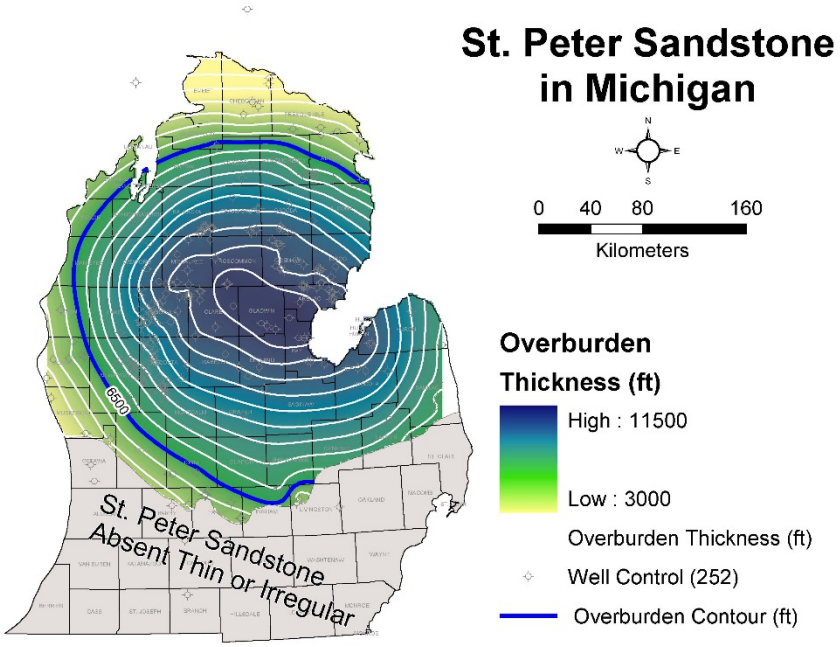

Figure 7. Overburden thickness (driller's depth) map of the St. Peter Sandstone in central and northern Lower Michigan. Although composite Paleozoic Michigan basin subsidence was multi-stage (see text for discussion) the predominant signal is basin subsidence centered on the "mitten" of the Lower Peninsula. Depth contours are 500 ft. The effective zero isopach parallels the Findley arch, although isolated outliers of St. Peter Sandstone are present in several wells to the south of this irregular line.

Barnes and others (1992) presented the results of detailed stratigraphic, sedimentologic and petrologic analysis of the St. Peter Sandstone on the basis of integrated, conventional core and wireline log studies in the Michigan basin subsurface. This work indicates that the formation consists of, from base to top, (1) up to 250 m of sandstone deposited in intertidal and supratidal sand flats and possible marine reworked aeolian deposits with associated dolomitic lagoonal deposits, and shallow subtidal shoreface environments, (2) sandstones deposited in subtidal shoreface to upper offshore environments, and, (3) dolomitic and argillaceous sands deposited in a more distal, storm-dominated epieric sea setting (see also: Dott, and others, 1986; Drzewiecki, and others, 1994; Stonecipher, 2000; Zdan, 2013).

An important approach used in this study is the calibration of wire-line logs with conventional core analysis data. Conventional core to (modern) log calibration/correlation facilitates the discrimination of sedimentary lithofacies and reservoir properties in logs in order to improve the reliability of CO_2 SRE. A type, modern well log section (Figure 8) from the central Michigan basin is shown from the Hunt Martin (P# 35090, Gladwin Co., MI). A regional, west to east stratigraphic cross section (reference is top Glenwood), including this well, is shown in Figure 9. Three south to north stratigraphic cross sections in central Lower Michigan are shown in Figure 10-12. Regional stratigraphic and paleogeographic relationships in the St. Peter Sandstone in the Michigan basin supported by these cross sections include:

1) Regional stratigraphic pinch out to the south,
2) Increased formation thickness from this pinch towards the north, in the basin center (refer to Figure 6 and 7),
3) Decrease in gamma ray log response towards the north and west throughout the St. Peter suggesting a (modern) northwesterly sand source,
4) Carbonate-prone strata in the St. Peter increase, especially in the lower part of the section, towards the (modern) south and east in the basin suggesting a more distal depositional setting in this direction relative to clastic sediment sources to the (modern) north and west,
5) A distinct “lower” St. Peter is present in most areas of the basin and is identified on the basis of abundant primary carbonate (now dolomite) inter-beds and other subtle log response characteristics. The “lower” St. Peter is distinct relative to superjacent strata, which possess generally higher gamma ray log response (in sandstone lithofacies) but generally lower

carbonate content in the “upper” St. Peter. The “upper” St. Peter pinches out to the north and west in the basin towards the clastic sediment source,

6) More distal marine facies in the Glenwood formation are transitional downwards to the “upper” St. Peter (Barnes, and other, 1992) and thicken to the east in the basin in conjunction with higher gamma ray log response in the “upper” St. Peter. These relationships indicate an easterly dipping paleoslope into the central Michigan basin,
7) Although not clearly demonstrated in these sections, the St. Peter thins and losses more distal facies at the top of the formation in basin margin locations to the west, north, northeast, and east, suggesting an enclosed marine basin setting in Michigan during St. Peter time.

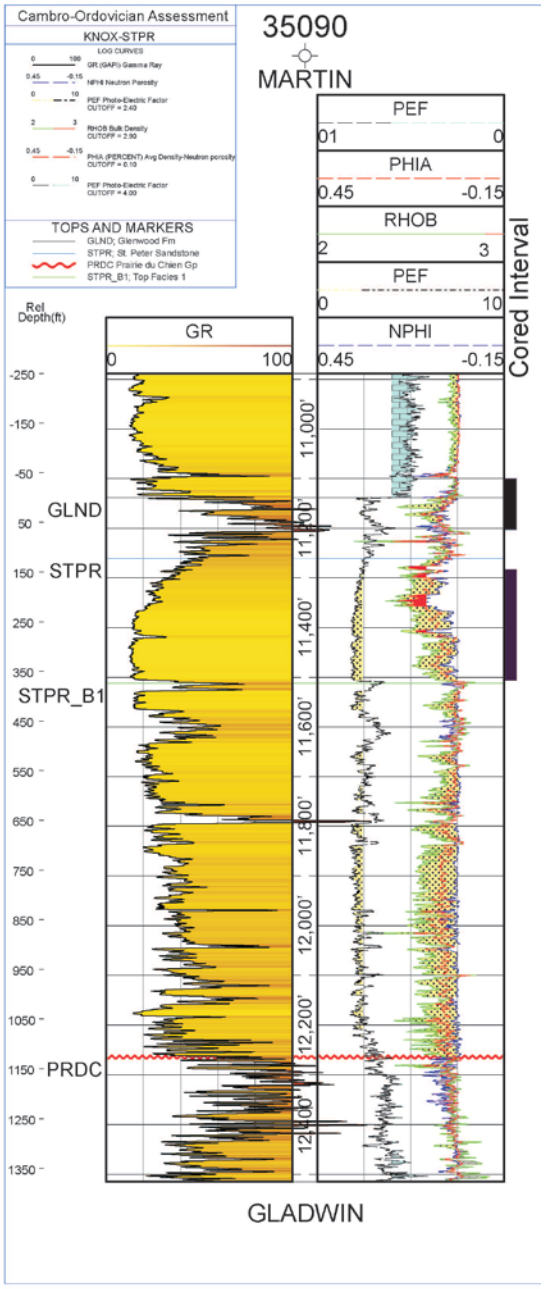

Figure 8. Well log display (GR, NPHI, RHOB, and PEF and shading are described in the legend) of the type log for the St. Peter Sandstone in the Michigan basin; Hunt Martin, Gladwin Co. Tops indicated (from base to top to the right of depth track) are Prairie du Chien)PRDC), “Lower” St. Peter Sandstone” (STTPR_B1), “Upper” St. Peter Sandstone (STPR), and Glenwood (GLND) formations. The characteristics used to identify these lithostratigraphic picks are described in the text. Dashed red log in track 2 is the average density and neutron porosity logs with a >10% cutoff shown with red shading.

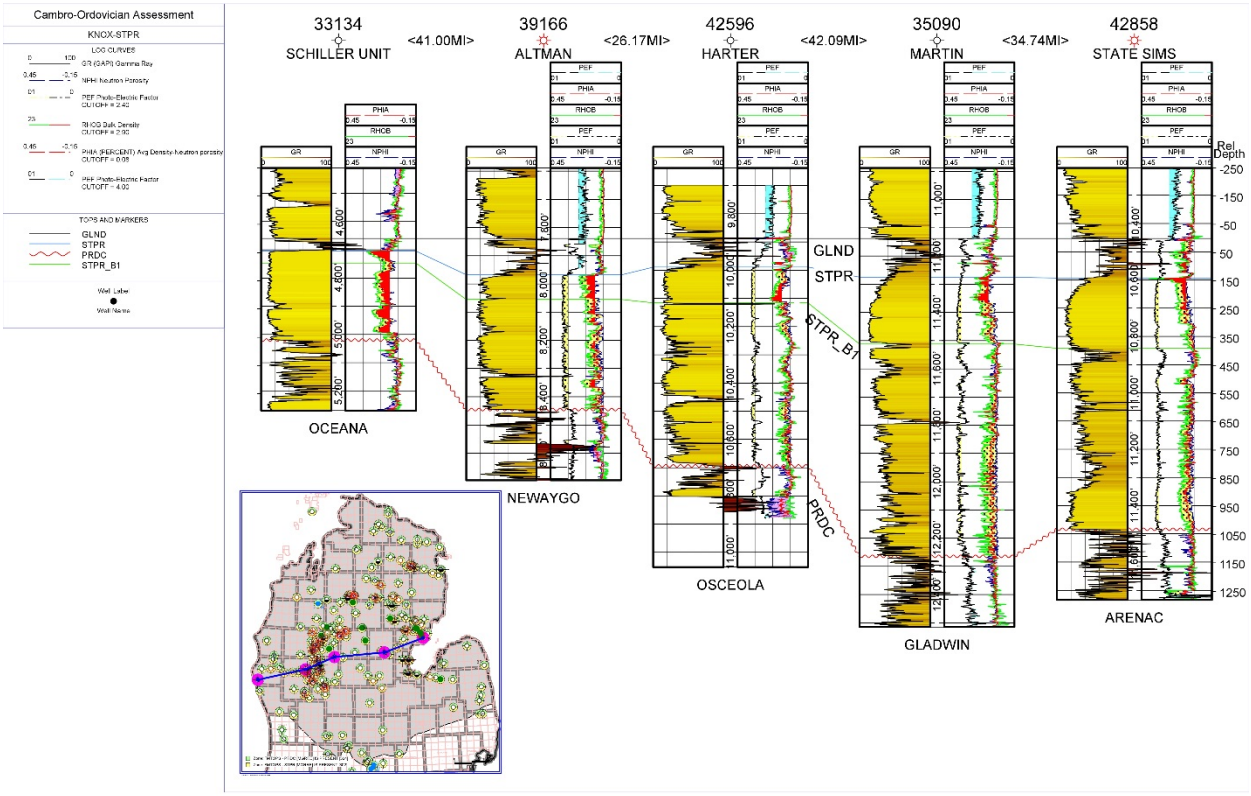

Figure 9. West to east MI Basin stratigraphic cross section showing internal reservoir facies subdivisions. Facies 1 predominates in the lower St. Peter (STPR_B1); Facies 3 & 4 occur in the upper St. Peter.

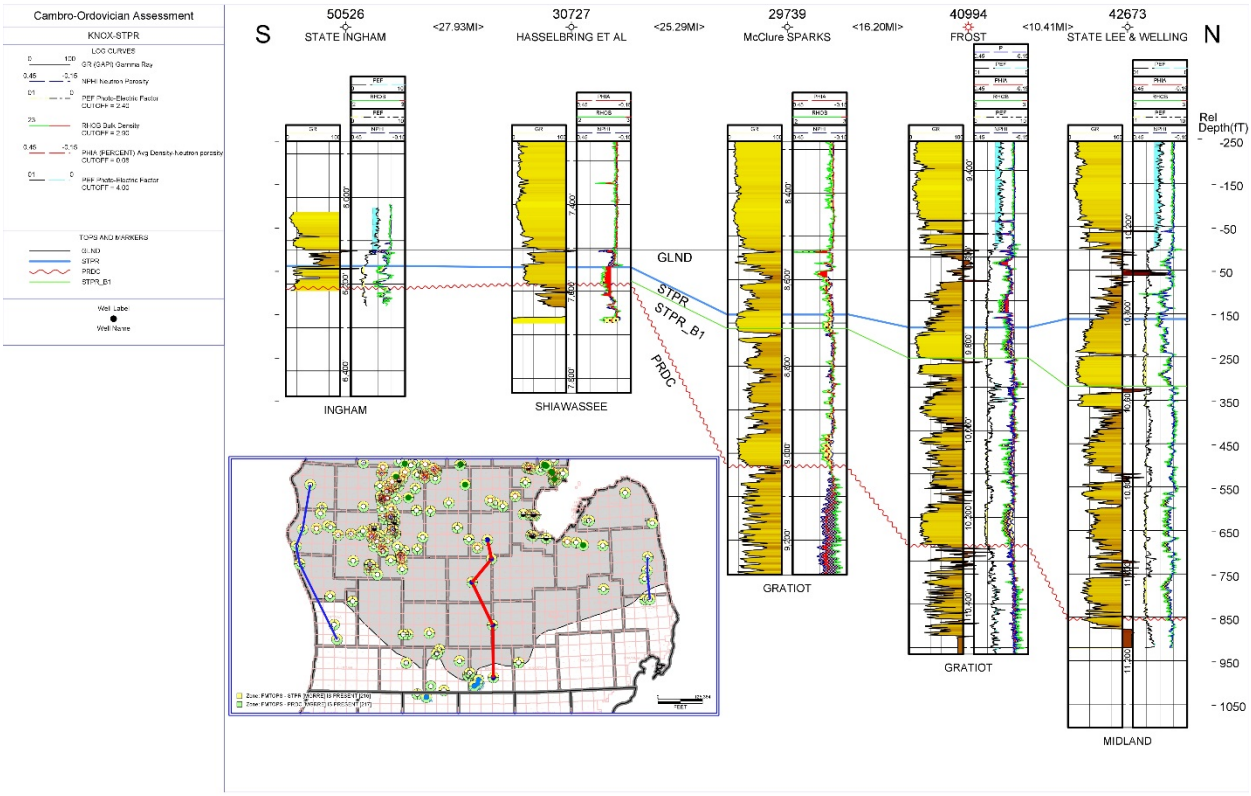

Figure 10. South to north MI Basin stratigraphic cross section (red section line) showing internal reservoir facies subdivisions. Facies 1 predominates in the lower St. Peter (STPR_B1); Facies 3 & 4 occur in the upper St. Peter.

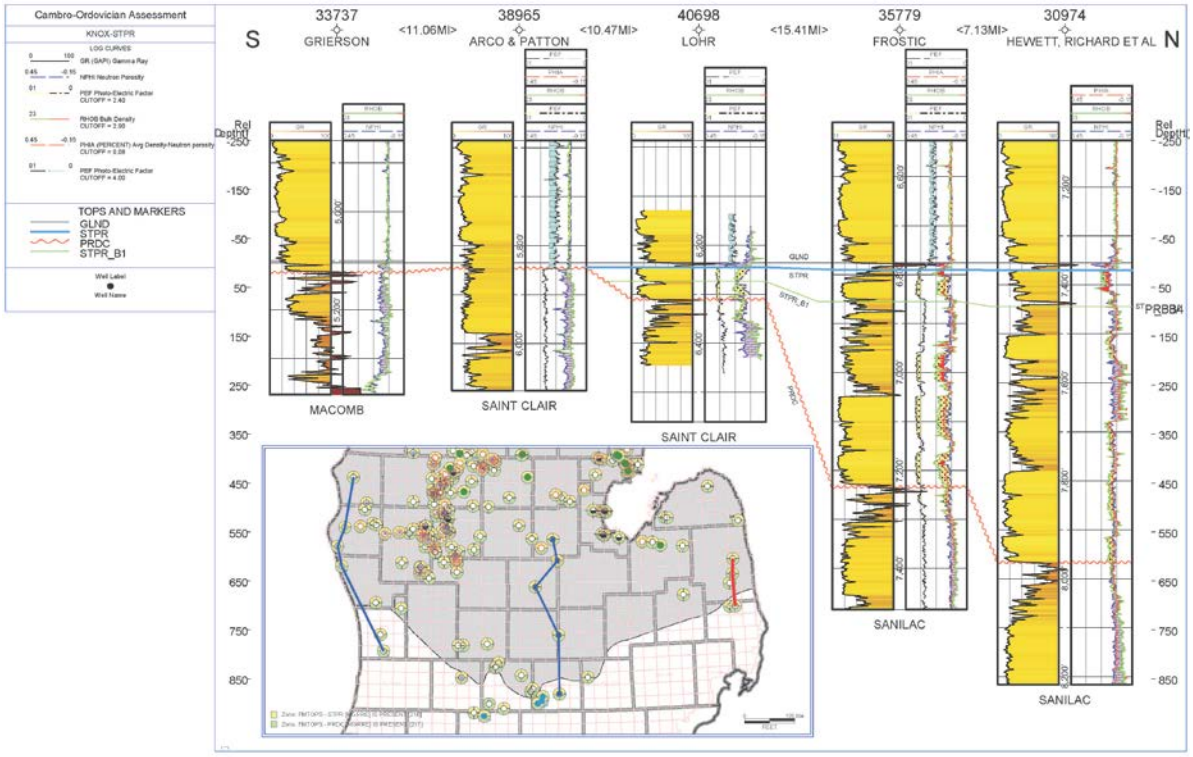

Figure 11. South to north MI Basin stratigraphic cross section (red section line) showing internal reservoir facies subdivisions. Facies 1 predominates in the lower St. Peter (STPR_B1); Facies 3 & 4 occur in the upper St. Peter.

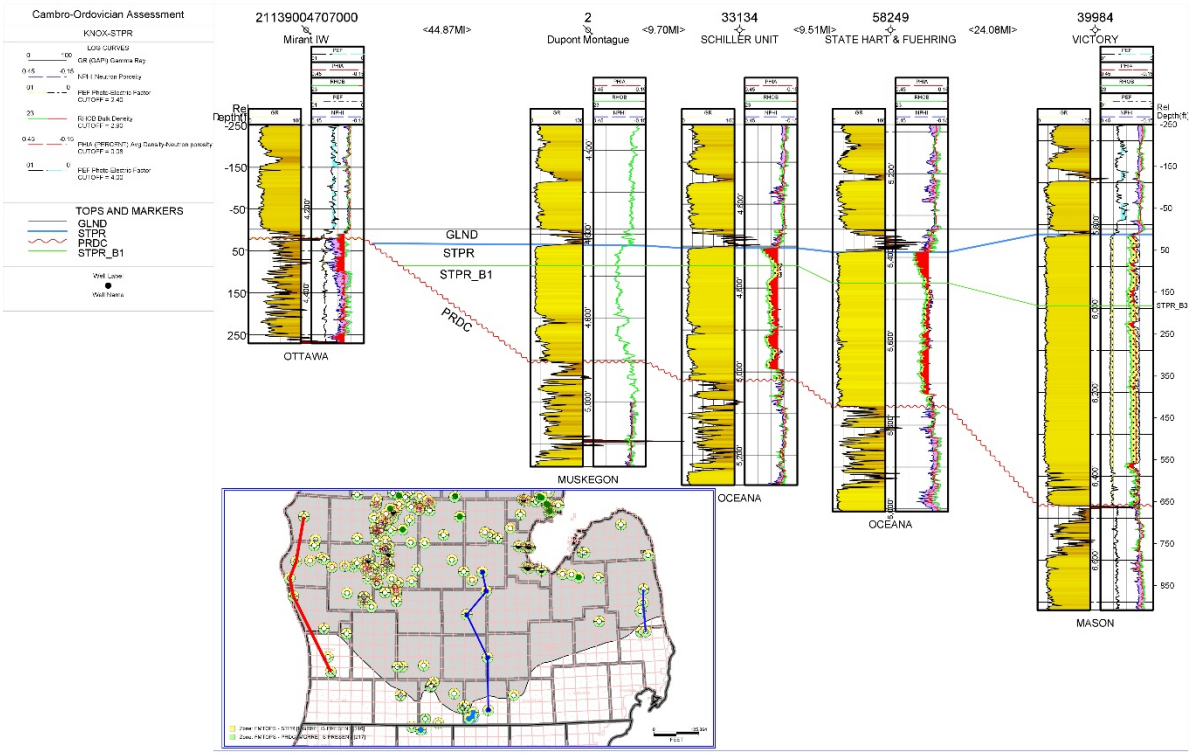

Figure 12. South to north MI Basin stratigraphic cross section (red section line) showing internal reservoir facies subdivisions. Facies 1 predominates in the lower St. Peter (STPR_B1); Facies 3 & 4 occur in the upper St. Peter.

Definition and Subsurface Expression of the St. Peter Sandstone in the Illinois basin

The St. Peter Sandstone occurs extensively throughout the Illinois portion of the Illinois Basin (Figure 2) including surface outcropping in the northern portion of the state where it is mined commercially for the production of Ottawa silica sand. Throughout the Indiana and Kentucky portions of the basin, variable deposition atop the Knox Supergroup along the regionally significant Knox unconformity (Figure 4) and lithofacies transition to carbonate-rich strata of the Ancell Group have led to some uncertainty as to the placement of the zero line of deposition. Prior work by Barnes and others (1992; Figure 2) and Pitman and others (1997) mapped the St Peter as extensive throughout Indiana, whereas Droste and others (1982) and Kolata (1992) suggest the St Peter Sandstone is more conservatively confined to the western half of Indiana and the Rough Creek graben region of western Kentucky. In this study we analyzed cuttings samples and wire-line log data from numerous wells throughout Indiana and western Kentucky to define the boundary for continuous occurrence of the St Peter where it meets the 800 meter depth criteria for consideration as a GCS reservoir (Figure 13). Isolated occurrences of St Peter are likely to be encountered to the east of our boundary line, but their highly variable extent (Droste and others, 1982) and shallower than 800 m depth effectively eliminates such occurrences for consideration in our SRE calculations.

Thickness of the St Peter Sandstone is highly variably owing to its deposition along the regionally significant and extensive Knox unconformity. Thickness of 100 m or more can be found in the northern portions of the Illinois Basin, however, shallow depths and ambient fluid chemistry with less than 10,000 ppm TDS preclude the potential use of the St Peter as a GCS reservoir in that region. Thickness of the formation generally declines eastward and southward throughout the basin (Figure 14) although the cross section shown in figure 15 illustrates how the St Peter may provide a viable GCS reservoir in the southern portions of Illinois where the Mount Simon Sandstone may be absent or thin, or otherwise unsuitable as a GCS reservoir.

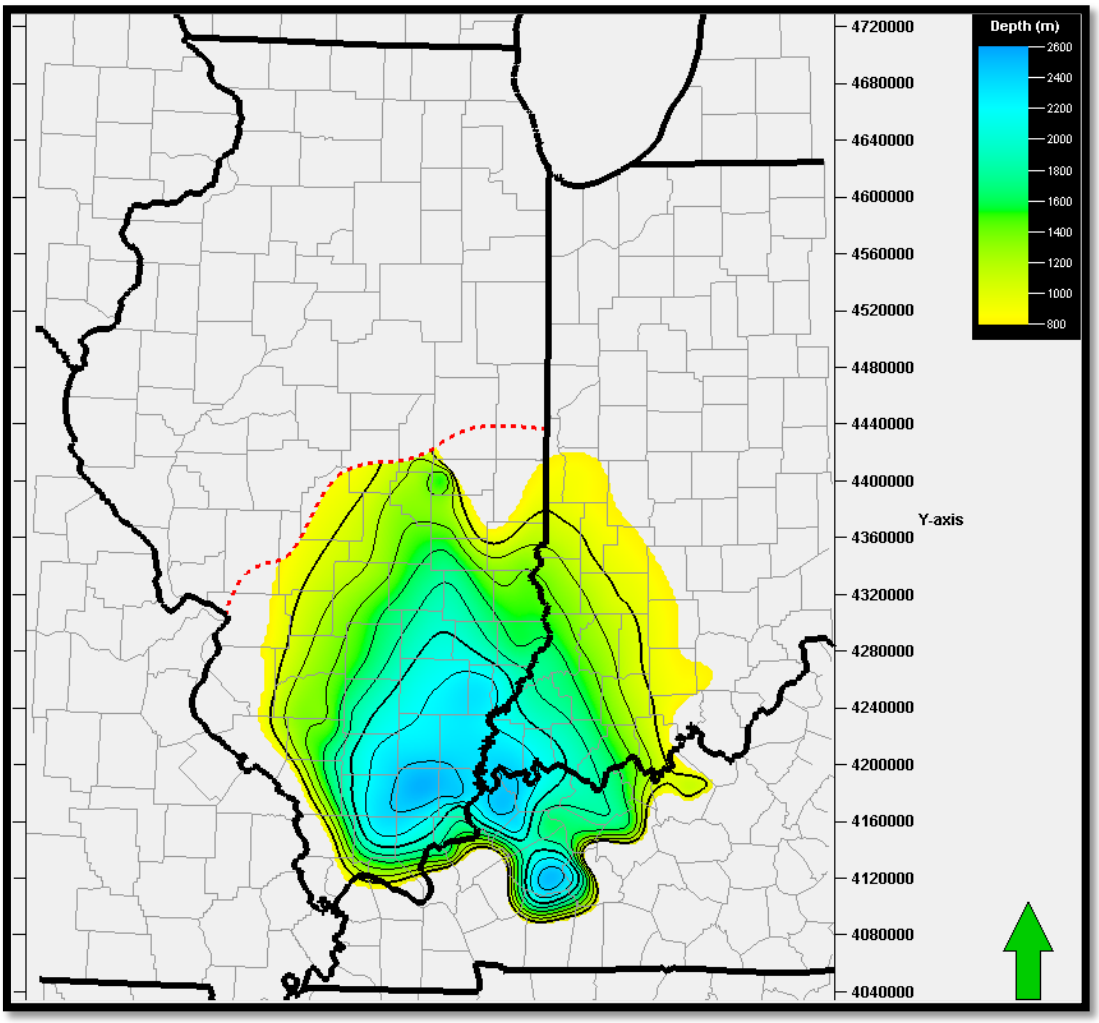

Figure 13. Overburden thickness map for the St Peter Sandstone in the Illinois Basin where depth to the top of the formation is greater than 800 m. Contour interval is 200 m. Maximum depths of approximately 2.5 km occur in the basin depocenter and structural grabens in western Kentucky. Dashed red line is the 10,000 ppm TDS line (Figure 5; USGS, 1995) defining the boundary for suitability as a GCS reservoir according to EPA UIC regulations.

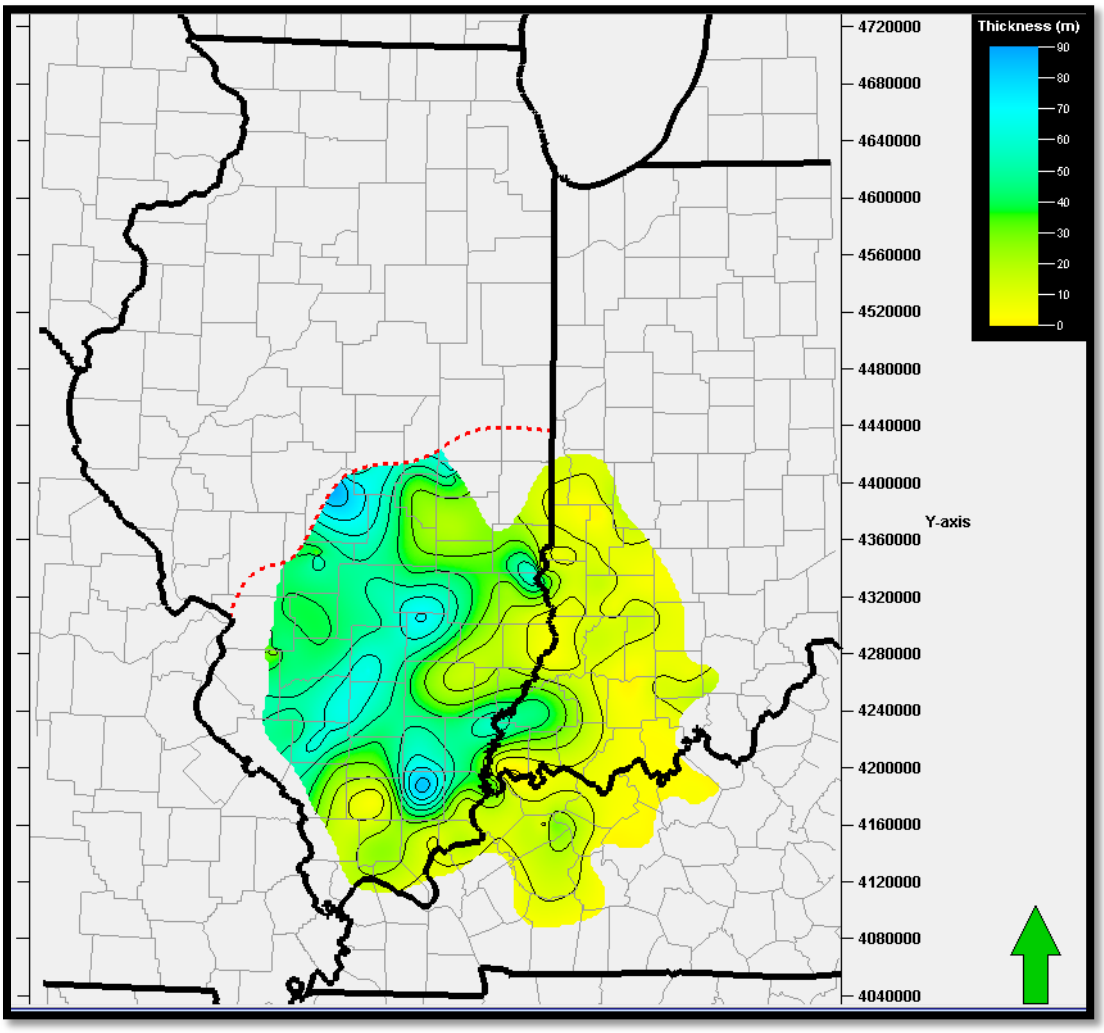

Figure 14. Thickness map of the St Peter Sandstone in the Illinois Basin throughout the potential GCS reservoir domain boundary. Thickness is relatively variable with intervals in excess of 50 m occurring in the Illinois portion of the basin. Contour interval is 10 m.

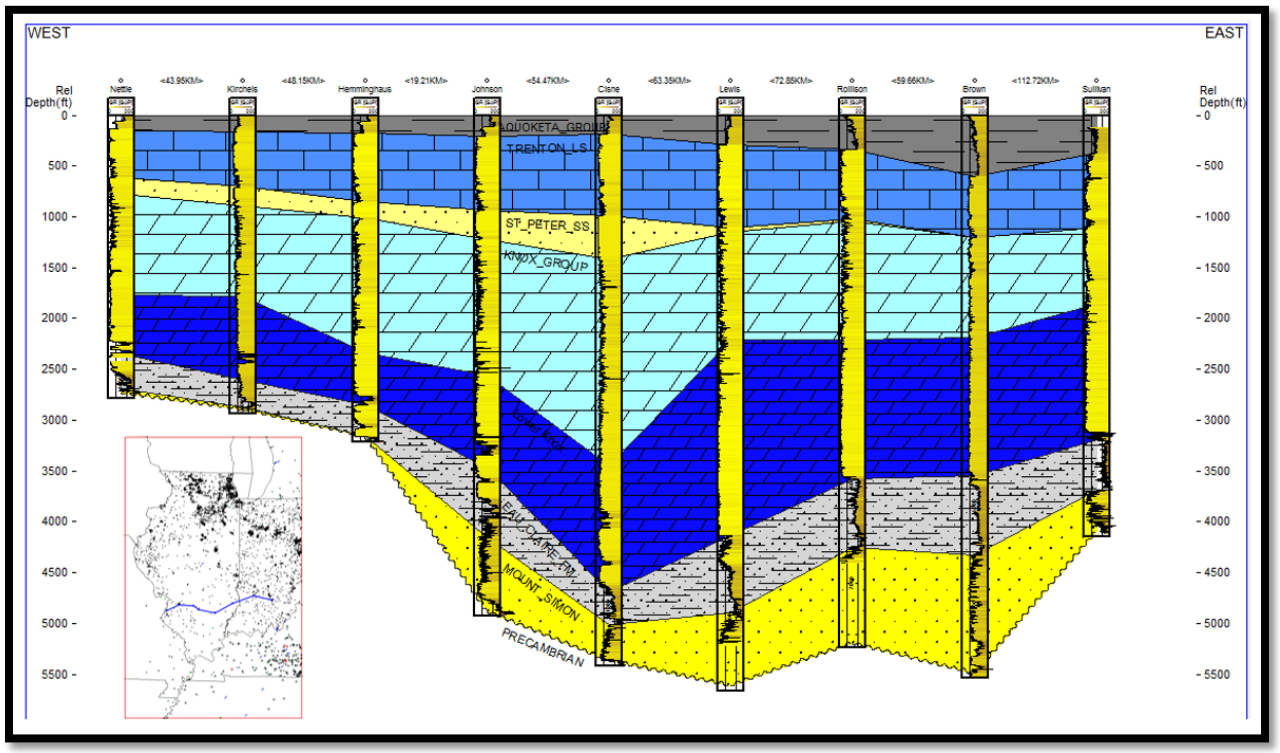

Figure 15. West-to-East cross section of the Cambro-Ordovician strata in the Illinois Basin illustrating the potential of the St. Peter Sandstone (light yellow) to provide a reservoir for CO_2 storage in southern Illinois where the Mount Simon Sandstone is very thin, absent, or otherwise unsuitable for CO_2 injection.

SRE for the St. Peter Sandstone in the Michigan and Illinois Basins

Saline formation CO_2 storage resource estimating is presented here in accordance with methodology presented by Goodman, and others (2011). The fundamental expression used in this methodology is expression 1:

$$GCO_2 = A_t h_g \emptyset_{tot} \rho E_{saline}$$

The total area (A_t), gross formation thickness (h_g), and total porosity ($\emptyset_{tot}$) terms account for the total bulk volume of pore space available. The CO_2 density (ρ) converts the reservoir volume of CO_2 to mass. The storage efficiency factor (E_{saline}) reflects the estimated fraction of the total pore volume that will be occupied by the injected CO_2 and include the CO_2 sequestration and displacement efficiency components. Various sources of data for the estimation of total bulk volume of pore space can be used depending on the available data in any area of investigation and Goodman, and others (2011) describe methods to determine storage efficiency factors over 10%, 50%, and 90% (P_{10}, P_{50}, P_{90}) probability ranges depending on the nature of data used for determination of total bulk volume of pore space. Volumetric methods for SRE in the St. Peter assume that the formation is an open flow system and that formation fluids would be displaced from the formation and CO_2 entrapment would be primarily the result of residual/capillary entrapment.

SRE in the Michigan Basin Using Area, Gross Thickness, Average and Depth Dependent Porosity

The St. Peter Sandstone is a predominantly saline aquifer unit in the Michigan basin with salinity values well in excess of 10,000 ppm TDS in all wells measured to date (pers. comm., Ray Vugrinovich, Michigan Office of Oil, Gas, and Minerals, working subsurface data base). Although significant hydrocarbon production is on-going in the basin, SRE presented here have not considered overlap with the areas of commercial hydrocarbon production. The areal extents of hydrocarbon producing structures in the basin are minor relative to the areal extent of the saline reservoir.

Initial SRE for the St. Peter Sandstone were determined using general geological data inputs to expression 1. Geographic information systems (GIS) software was used in conjunction with St. Peter isopach, overburden thickness, and formation porosity data from well logs to map and calculate the total bulk volume of pore space parameters; total area, formation thickness, and total porosity. This

product was then incorporated into the SRE expression using a CO_2 density (ρ) of 0.7 gm/cc and P_{10}/P_{90} storage efficiency factors (E_{saline}) appropriate for uncertainties with respect to net-to-total area $E_{An}/_{At}$, net-to-gross thickness $E_{hn}/_{hg}$, and effective-to-total porosity $E_{\phi e/\phi to}$ inherent to this data set (Goodman and others, 2011). Average formation porosity was established by determining the average porosity from neutron porosity/density porosity logs from 214 complete St. Peter Sandstone penetrations (Figure 16). **SRE calculated using this approach are P_{10} = 3.3 billion tons (Gt) and P_{90} = 35.1 Gt** (Figure 17).

Geological investigations in many basins and specifically in Paleozoic rock strata of the Midcontinent region (e.g., Medina and others, 2011) suggest a regular reduction in porosity with depth due to burial induced physical compaction and chemical cementation. As such, this analysis considered the relationship between depth of burial and porosity (Figure 16) to establish a functional relationship predicting porosity on the basis of depth. Using this trend (log function shown in Figure 16) a depth dependent porosity grid was created, and in conjunction with isopach data, provides the total porosity ($Ø_{tot}$) term for the total bulk volume of pore space calculation. As above, appropriate storage efficiency factors were used to calculate **SRE of P_{10} = 3 GT and P_{90} – 31.6 Gt** (Figure 18).

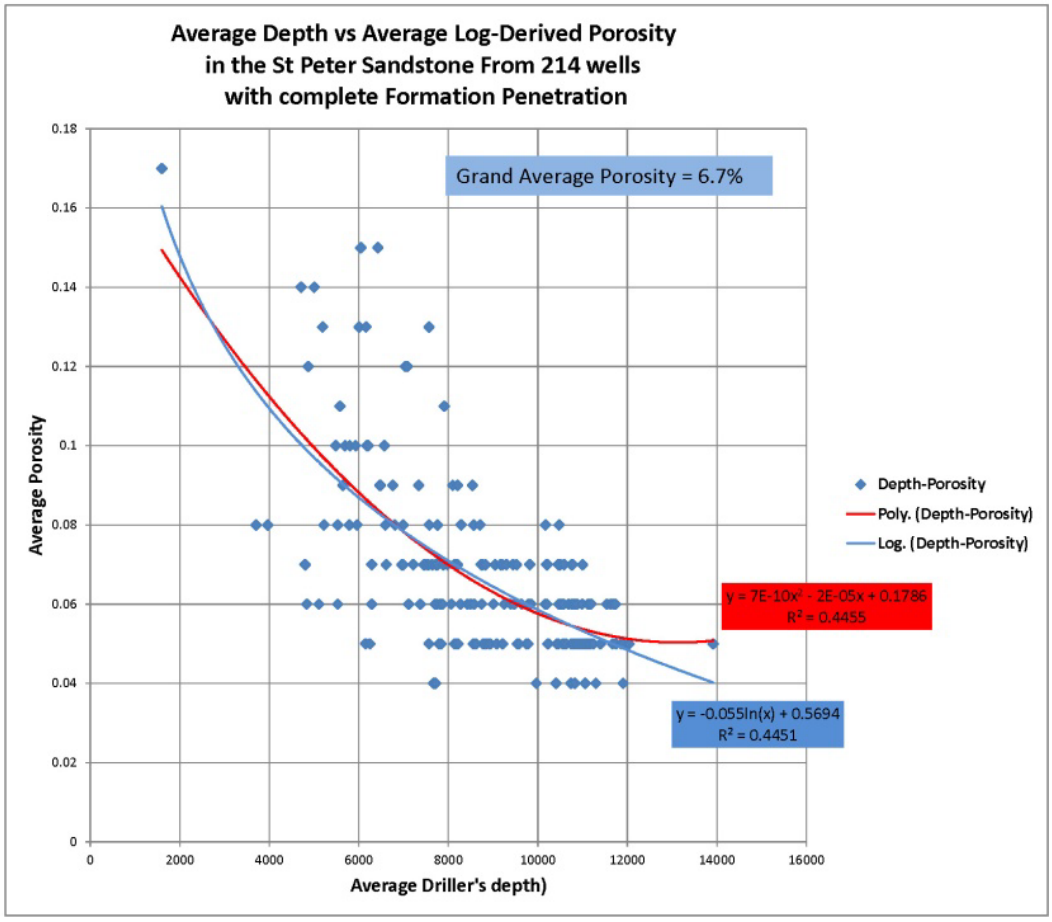

Figure 16. Plot of log derived average porosity (per well) versus average depth of the St. Peter Sandstone. Grand average porosity for 214 complete penetrations of the St. Peter Sandstone is 6.7% ϕ.

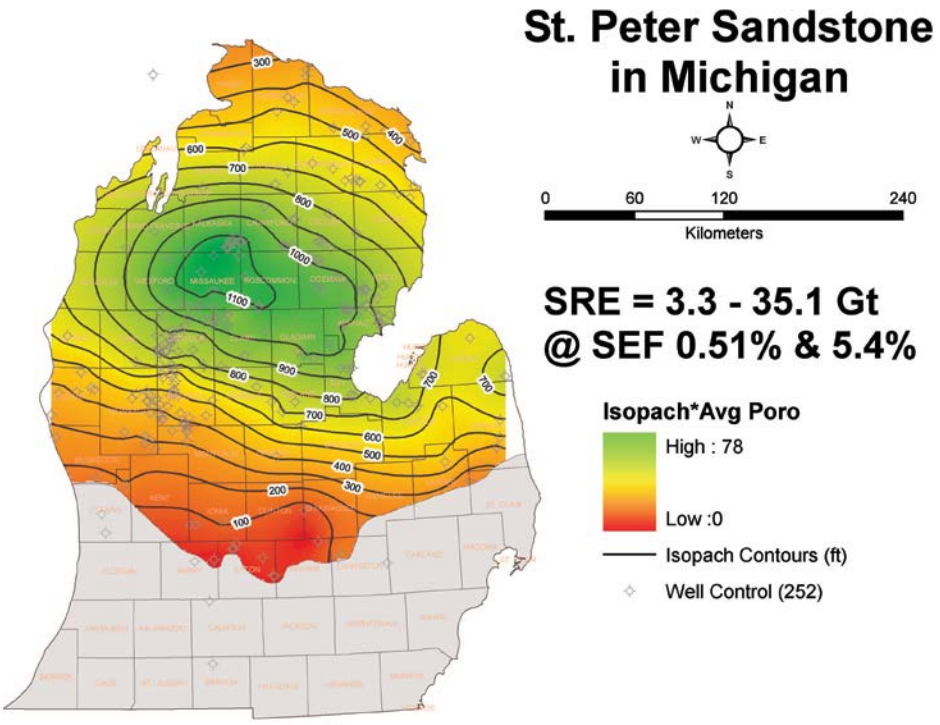

Figure 17. Total pore volume grid for Michigan using St. Peter Sandstone Isolith (h_g), area (A_t, in square kilometers), and average porosity (ϕ_{tot}; 6.7%). This product was then incorporated into the SRE expression using a CO_2 density (ρ) of 0.7 gm/cc and P10/P90 storage efficiency factors (E_{saline}) of 0.51/5.4%.

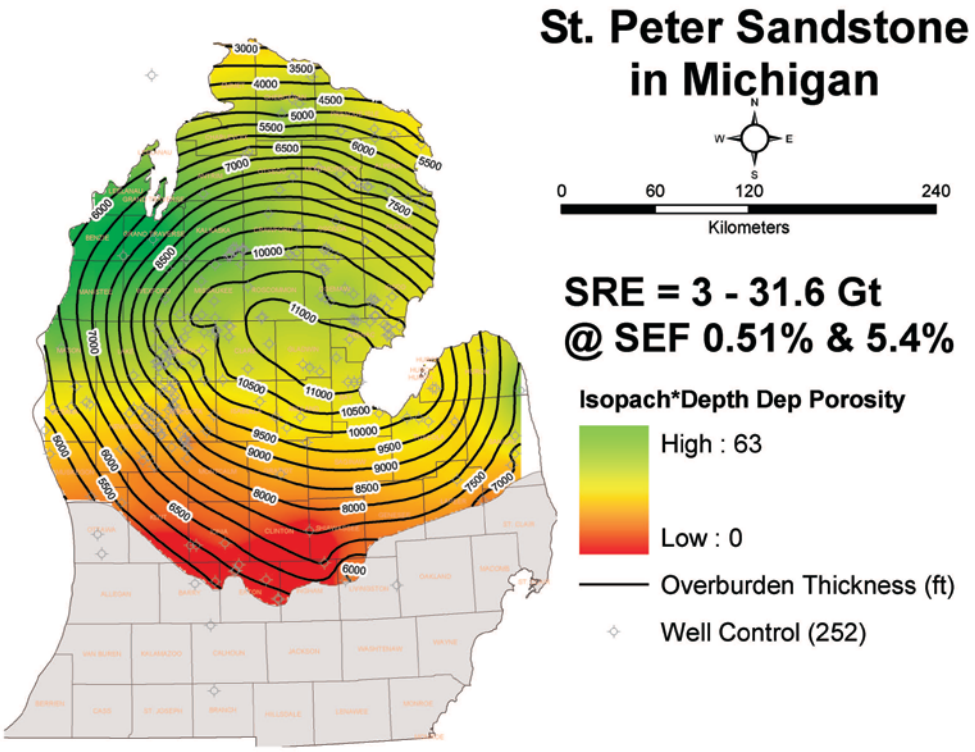

Figure 18. Total pore volume grid for Michigan using St. Peter Sandstone Isolith (h_g), area (A_t, in square kilometers), and depth dependent porosity (see text for discussion). This product was then incorporated into the SRE expression using a CO_2 density (ρ) of 0.7 gm/cc and P10/P90 storage efficiency factors (E_{saline}) of 0.51/5.4%.

SRE in the Illinois Basin Using Area, Gross Thickness, Average and Depth Dependent Porosity

Initial SRE calculations for the St Peter in the Illinois Basin were performed in the same manner as outlined in the prior section for the Michigan Basin with the exception that the average porosity (i.e., formation-level effective mean porosity) was estimated from the mean of all available core analyses sampled at 46 wells across the basin (n=2,421). Figure 19 shows the distribution of core analyses for which both porosity and permeability have been measured. The mean porosity from all available core plug analyses is 14.1% (n=2,421). Applying this value in equation 1 and assuming the same mean CO_2 density and efficiency factors as the prior case for the Michigan Basin resulted in **SRE values of 1.0 to 11.0 Gt for the P10 and P90 probability range, respectively**. Figure 20 shows the total pore volume grid (in units of porosity meters) associated with this SRE calculation and is analogous to figure 17 for the calculation of the Michigan Basin.

Similar to the findings reported earlier for the Michigan Basin and in several prior studies (e.g., Hoholick and others, 1984; Medina and others, 2011) porosity of the St Peter Sandstone was found to exhibit a generalized decline with depth despite local-scale heterogeneity in porosity of up to 30%. Early results of our analysis of the St Peter Sandstone were provided to the Midwest Geological Sequestration Consortium and were subsequently published in the NETL Atlas IV publication (2012) and the NATCARB database. Those results used a linear function of porosity decline with depth as an initial step to improving the prior published SREs that were based on the average formation porosity approach (Figure 21). Subsequent analysis of petrophysical properties and photomicrographs of newly available core from GCS study wells in Knox County, Indiana (Figure 22) and the Illinois Basin Decatur Project (Figure 23), as well as advanced wire-line log analysis of the CCS#1 and Verification #1 wells at IBDP (Leetaru and others, 2012) all demonstrated that the linear model tended to under-predict porosity with depth. Accordingly, a new exponential function was fit to the core data set to provide a better model of the depth dependency of porosity of the St Peter in the Illinois Basin (figure 24). Figure 25 shows the total pore volume grid associated with this SRE calculation and is analogous to figure 18 for the comparable calculation in the Michigan Basin. Application of the appropriate SEFs resulted in **the SRE range of 0.6 to 6.1 Gt for the P_{10} and P_{90} values, respectively.**

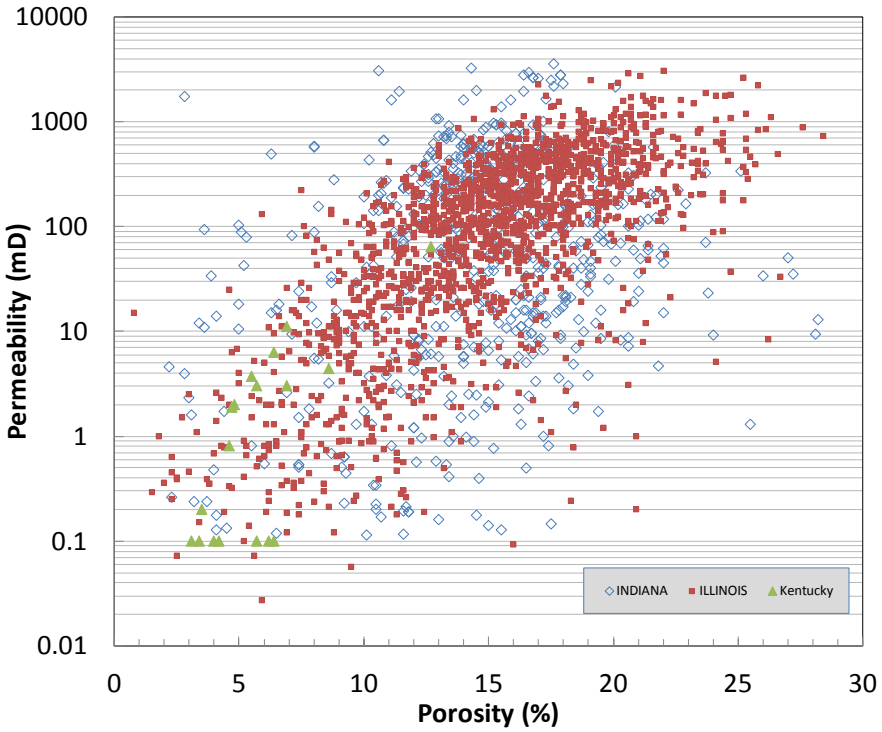

Figure 19. Cross plot of porosity with permeability of the St. Peter Sandstone in the Illinois Basin from 46 wells with conventional core plug analyses. The mean porosity from all core plug analyses is 14.1% (n=2,421). The mean permeability is 255 mD (n=558).

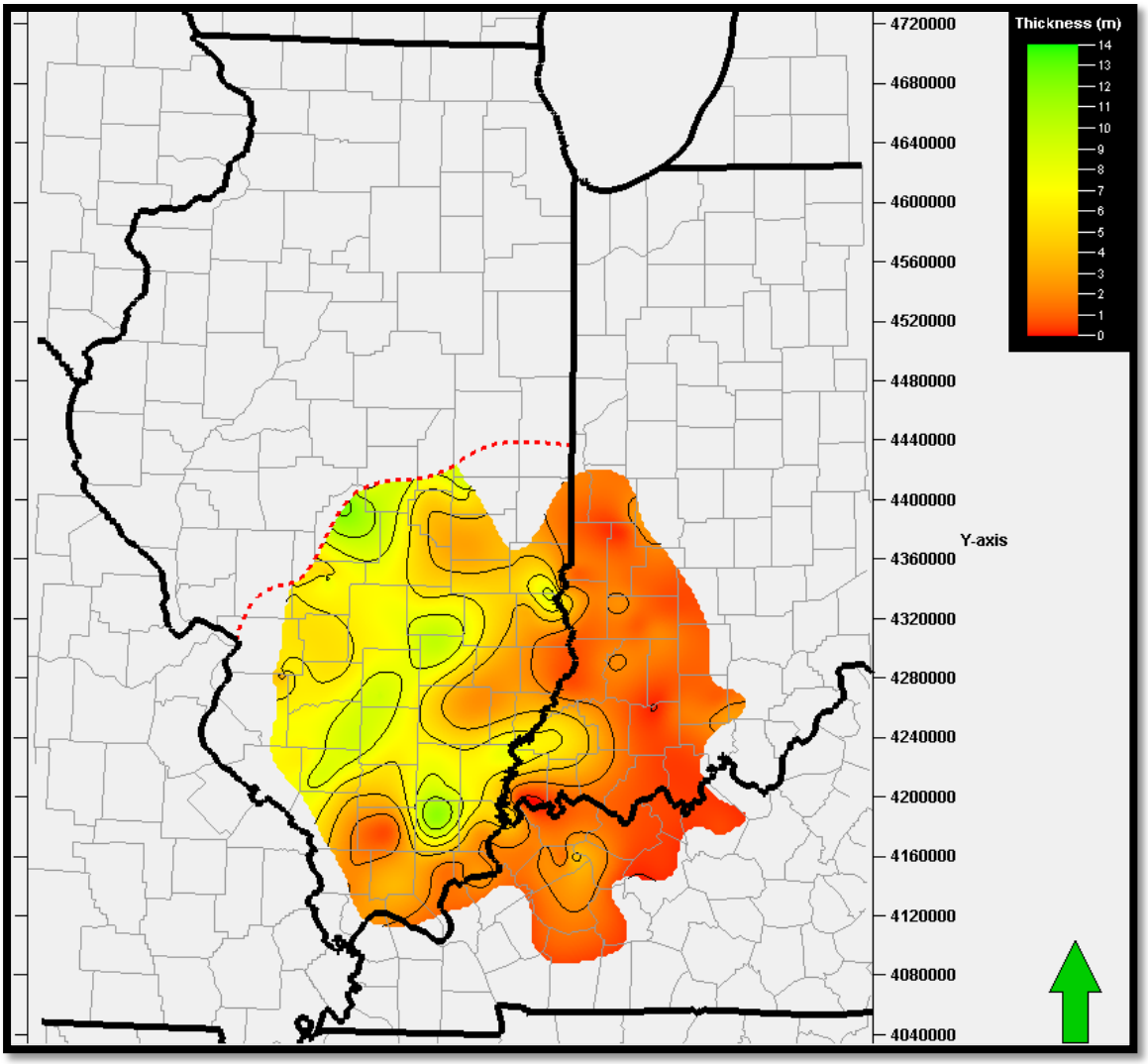

Figure 20. Total pore volume grid in the Illinois Basin using St. Peter Sandstone isopach (h_g), area (A_t, in square kilometers), and average porosity (ϕ_{tot}; 14.1%). Unit is thickness of total porosity in meters, ranging from 0 (red) to 14 m (green). This product was then incorporated into the SRE expression using a CO_2 density (ρ) of 0.7 gm/cc and P10/P90 storage efficiency factors (E_{saline}) of 0.51/5.4%.

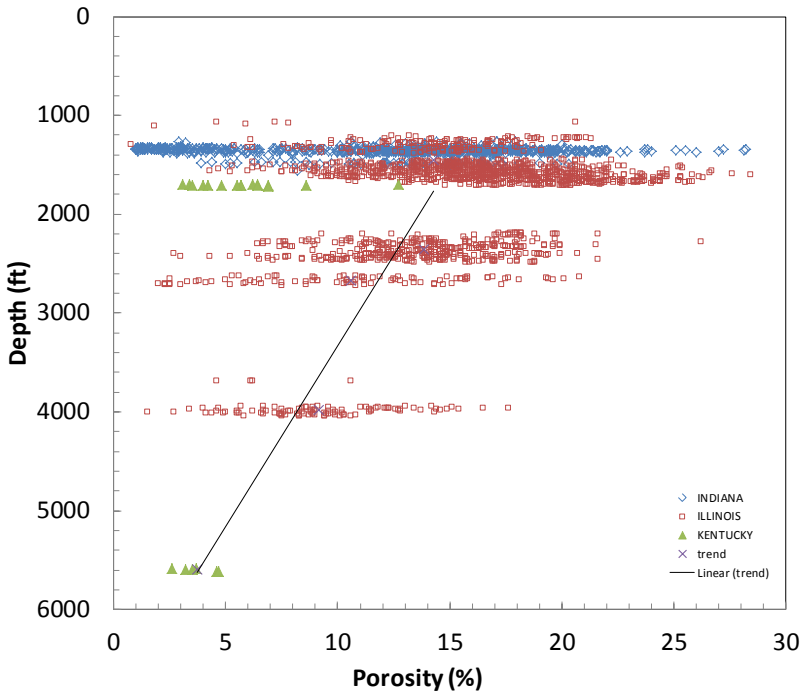

Figure 21. Spatial variability in porosity of the St. Peter Sandstone was initially modeled by using a depth-based linear function that was fit using regression against core analyses from all available wells and a minimum porosity threshold of 4% at depth. The resulting SREs were submitted to NATCARB in 2012 and published in the DOE Atlas IV (NETL, 2012).

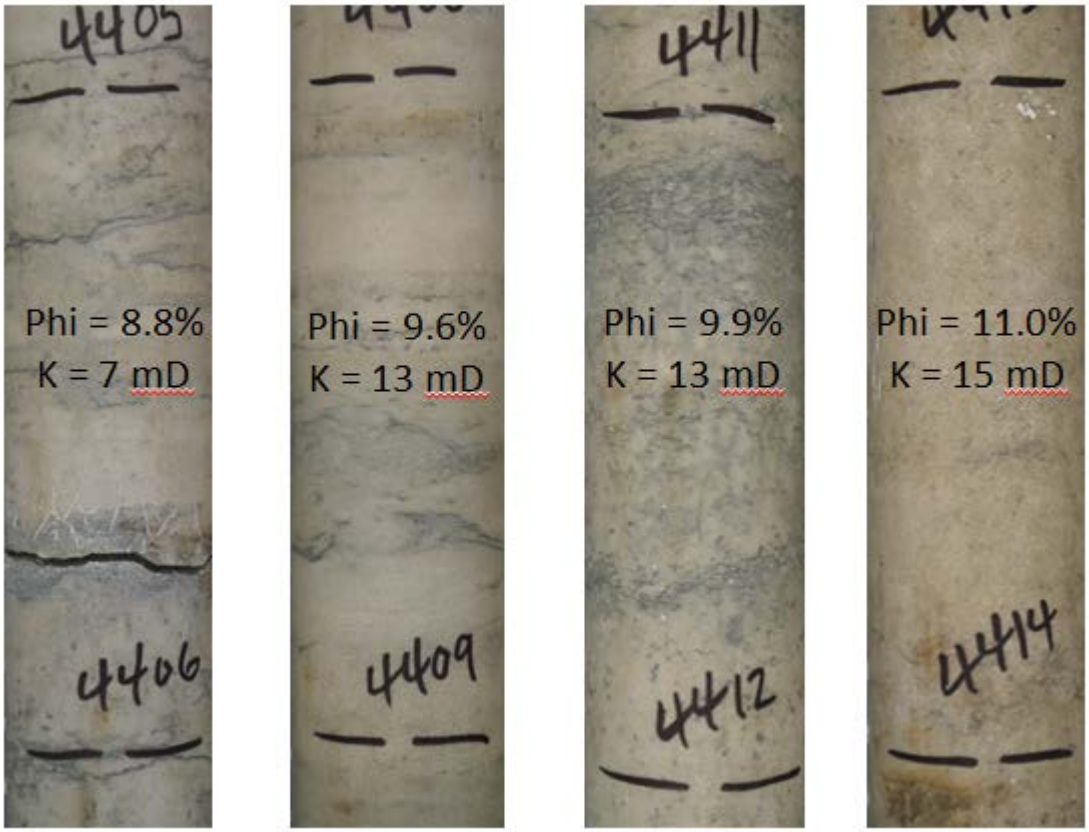

Figure 22. Assessment of the simple, linear depth-dependent porosity model from independent analyses of St Peter Sandstone core samples from Knox County, IN (Well ID 164778). The St Peter Ss Formation at this well is located within the potential reservoir domain of the Illinois Basin at depths of 1,341 to 1,346 meters (4,400 to 4,415 feet). The linear depth-based porosity function was shown to under-predict porosity with an estimate of 7.2%.

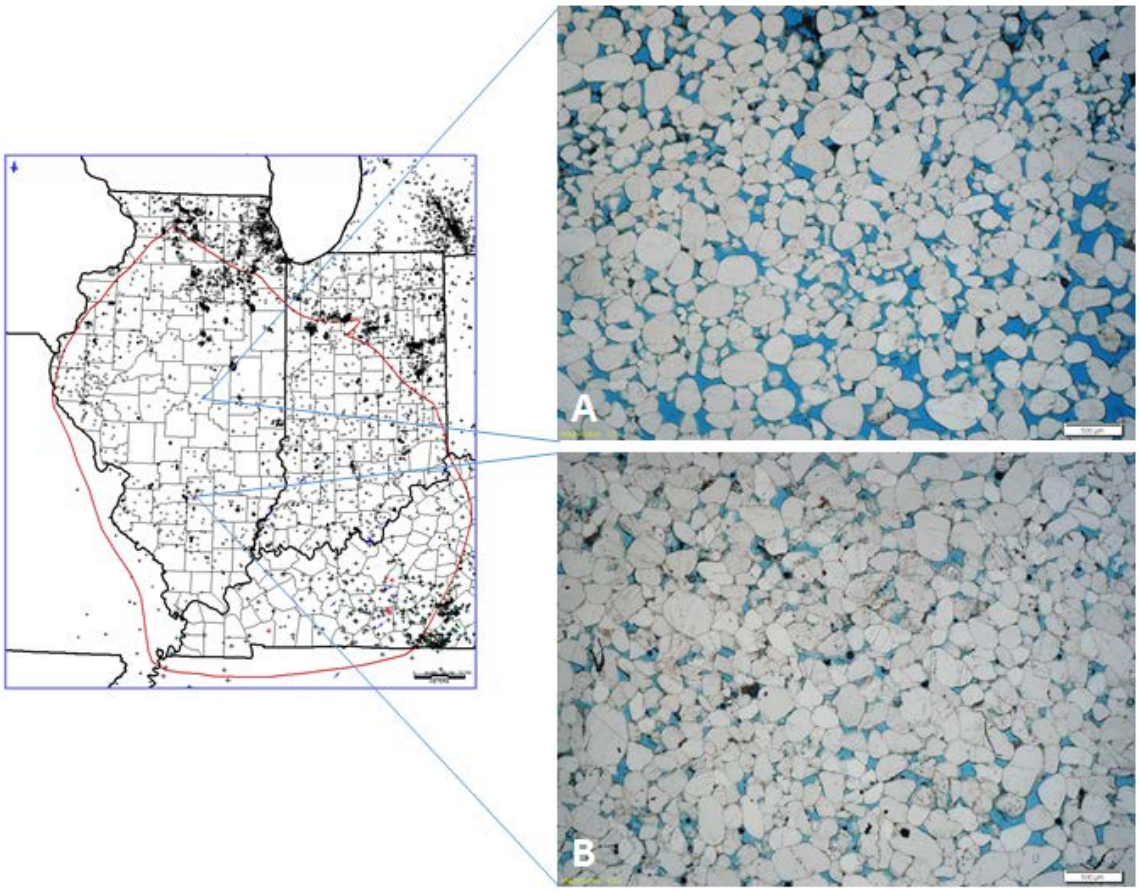

Figure 23. Photomicrographs of St Peter Ss core from the Illinois Basin illustrating diagenetic affects of compaction and cementation on porosity. (A) CCS#1 well in Decatur, IL; depth = 1,052 m (3,450 ft); porosity = 19.6%. (B) Johnson #1 well in Marion County, IL; depth = 1,600 m (5,249 ft); porosity = 11.6%.

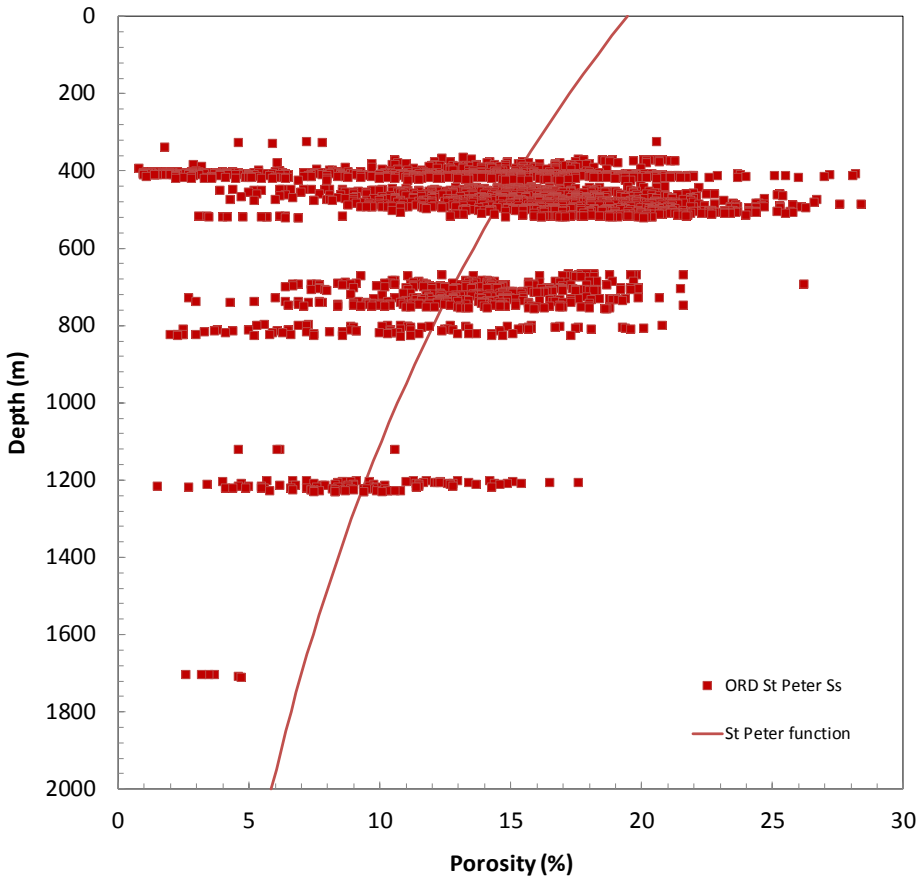

Figure 24. A generalized, depth-based model of porosity defined by the exponential function: porosity = $19.45e^{-6E-04z}$. Further assessment of the St Peter Sandstone throughout the Illinois Basin supports the use of this model for more accurate SRE calculations.

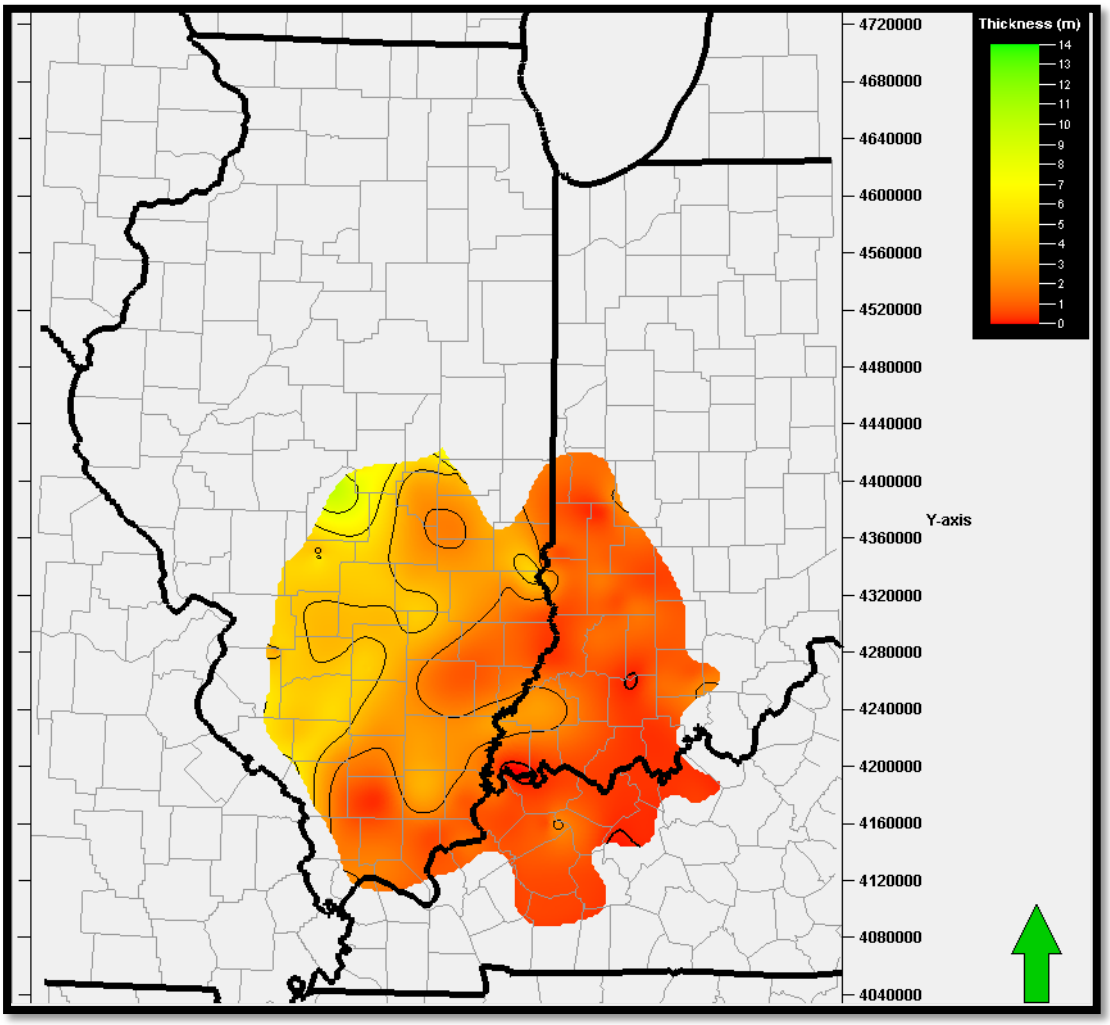

Figure 25. Total pore volume grid for the Illinois Basin using St. Peter Sandstone Isolith (h_g), area (A_t, in square kilometers) and the depth-based porosity model shown in figure 24. This product was then incorporated into the SRE expression using a CO_2 density (ρ) of 0.7 gm/cc and P10/P90 storage efficiency factors (E_{saline}) of 0.51/5.4%.

SRE in the Michigan Basin Using Area, and Net Thickness from Core and Log Data Analysis

Abundant conventional core and modern well log data from the St. Peter Sandstone in Michigan allow for less uncertain and therefore more precise SRE. Goodman and others (2011) suggest that if net-to-total area ($E_{An}/_{At}$), net-to-gross thickness ($E_{hn}/_{hg}$), and effective-to-total porosity $E_{\phi e}/_{\phi tot}$ are known, only a displacement efficiency factor is necessary for the SRE calculation. If a minimum effective porosity value can be established from conventional core data then that porosity cutoff value can be used in the analysis of effective porosity in the evaluation of individual porosity well logs.

A compilation of conventional core porosity and permeability data from 80 wells in the St. Peter Sandstone is presented in Figure 26. An exponential trend line through these data shows poor correlation coefficient suggesting a variety of influences on porosity characteristics. However, in order to establish a reasonable value for effective porosity, a minimum 5 millidarcy (md) value was chosen and this minimum effective permeability results, by the exponential transform, to 10.5%ϕ as minimum effective porosity. When this effective porosity cutoff value is used to screen porosity values from modern porosity logs a net porosity sum is generated for each well control point. A net porosity grid was then constructed (figure 27) to calculate total bulk volume of pore space used in the SRE expression. Because uncertainty with respect to total bulk volume of pore space parameters using this approach are ostensibly eliminated, displacement storage efficiency factors for P_{10} and P_{90} of 7.4% and 24% (respectively; Goodman and others, 2011) are applied resulting in **SRE of 10.7 Gt to 34.7 Gt**.

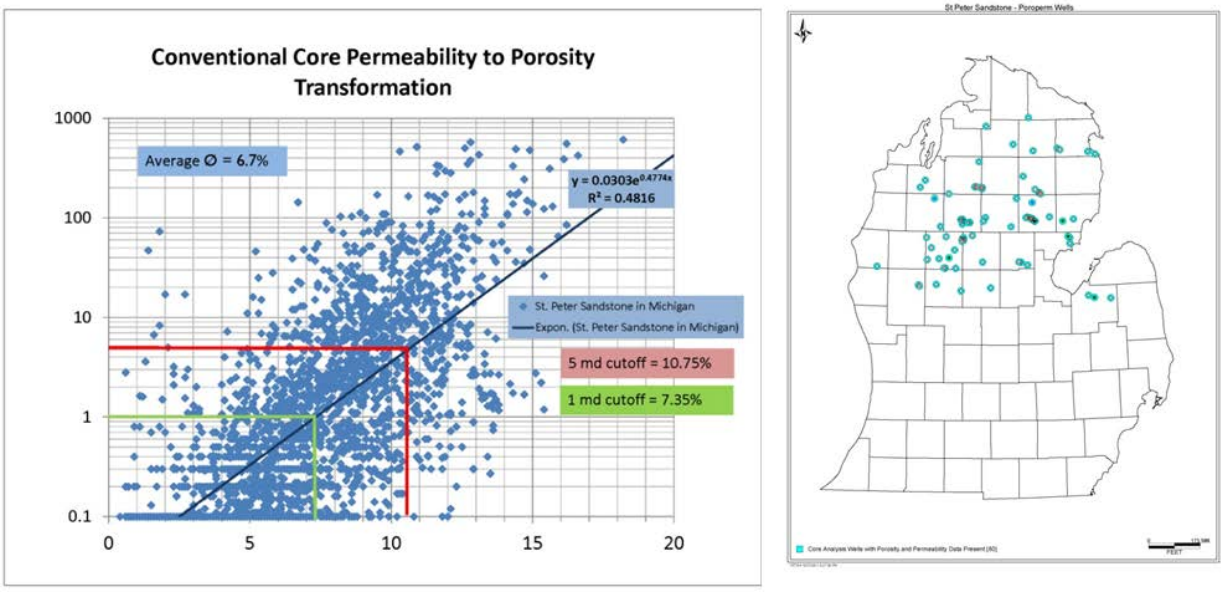

Figure 26. Left, Conventional core porosity versus permeability semi-log plot for the St. Peter Sandstone in the Michigan basin. Although the exponential trend line correlation coefficient is poor, a cutoff value for effective porosity using a 5 md minimum permeability is 10.5%ϕ. Interestingly, the grand average of porosity from over 2500 porosity-permeability measurements is 6.7%ϕ, the same value derived from porosity log analysis (Figure 16). Right; map showing the source of data for the plot, left, in 80 cored wells in the St. Peter Sandstone.

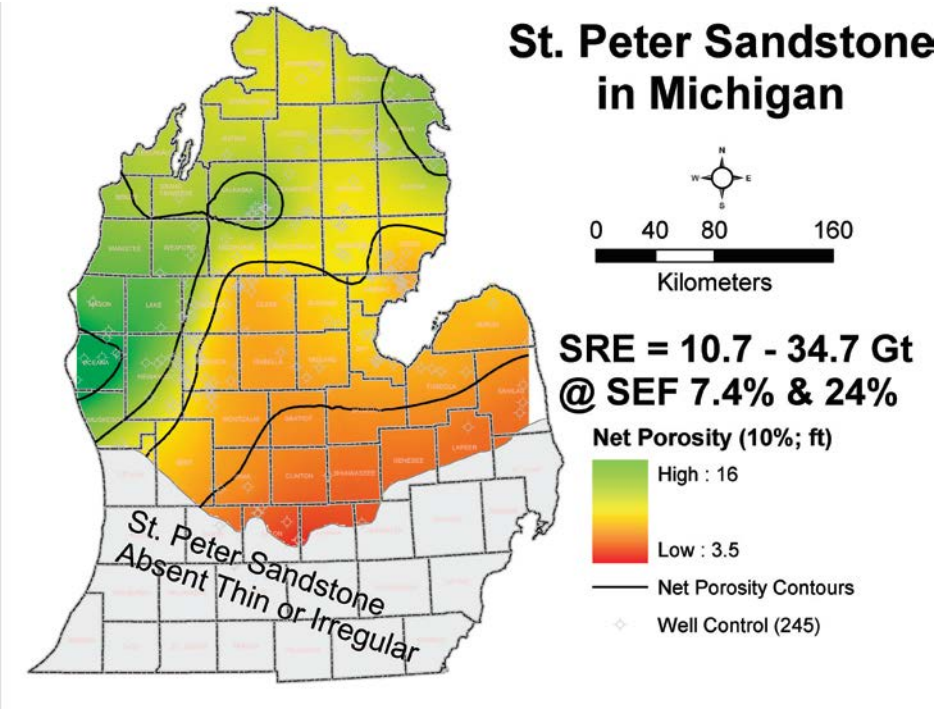

Figure 27. Net porosity grid derived from log analysis of net porosity for 245 control wells with modern porosity logs in the St. Peter Sandstone. Scale is in ft^3/ft^2. Location of control wells shown by well control symbols.

SRE in the Illinois Basin Using Area, and Net Thickness from Core and Log Data Analysis

Although the results presented in the prior section tend to substantiate the exponential decline in porosity of the St Peter with depth throughout the Illinois Basin, the depositional and diagenetic impacts on porosity are clearly more variable and complex than can be captured by a single generalized model such as the one given in figure 24. The basin-wide petrographic study of Hoholick and others (1984) indicated that primary porosity is generally dominant in the St Peter down to a depth of approximately 1,200 meters. These researchers found that below this depth, secondary porosity becomes dominant and the general chronology of porosity evolution involves early cementation, leaching of cement and framework, stabilized framework, and framework collapse. Later work by Pitman and others (1997) combined petrographic analysis with SEM, CL microscopy, fluid-inclusion microthermometry and other analyses to provide a more comprehensive picture of diagenesis throughout the basin. Their paragenetic sequence and regional mapping of cements illustrates the complex diagenetic history of the St Peter, including multiple episodes of primarily carbonate cement dissolution in the deeper, southern portion of the basin resulting in secondary porosity formation.

Given this inherent regional variability in porosity, another SRE was calculated following the net porosity thickness approach discussed previously for the Michigan Basin. The primary difference between our analysis in the Illinois Basin and the Michigan Basin is the substantially more limited wire-line log data set available throughout the potential reservoir domain. Our analysis of the Illinois Basin was based on neutron porosity logs from 32 wells across the basin. A statistically significant correlation between porosity and permeability was found for the core samples from the Illinois portion of the basin (the dominant region of potential storage) and assuming a permeability threshold of 5 mD resulted in a porosity cutoff value of 7% (Figure 28). The resulting net porosity grid is shown in figure 29, indicating a more favorable region of potential storage resource in the western portion of the domain than did the prior analysis (figure 25). Application of the displacement only SEFs resulted in significantly larger **SREs of 11.2 to 36.4 Gt for the P10 and P90 values**.

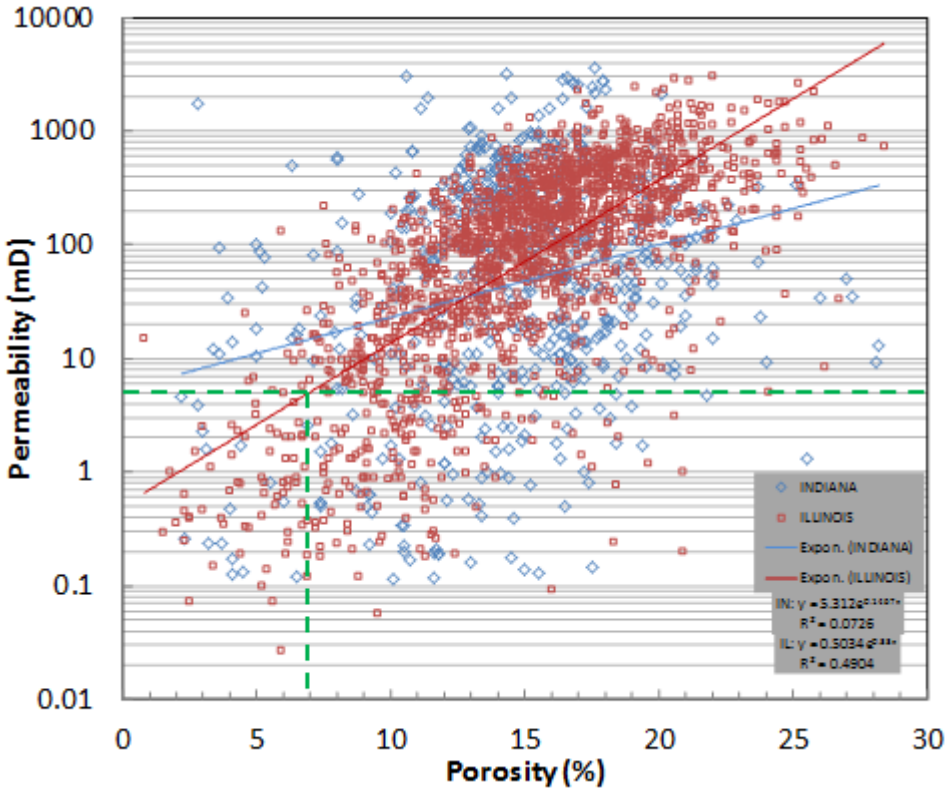

Figure 28. Core analyses indicate a meaningful correlation between porosity and permeability in the Illinois State region (R2 = 0.5) with a mean porosity of 15.0% and a mean permeability of 235 mD. A reservoir cutoff of 5 mD correlates to 7.0% porosity. This cutoff value was applied to available well logs in the reservoir domain to calculate SRE based on an explicit net porosity evaluation.

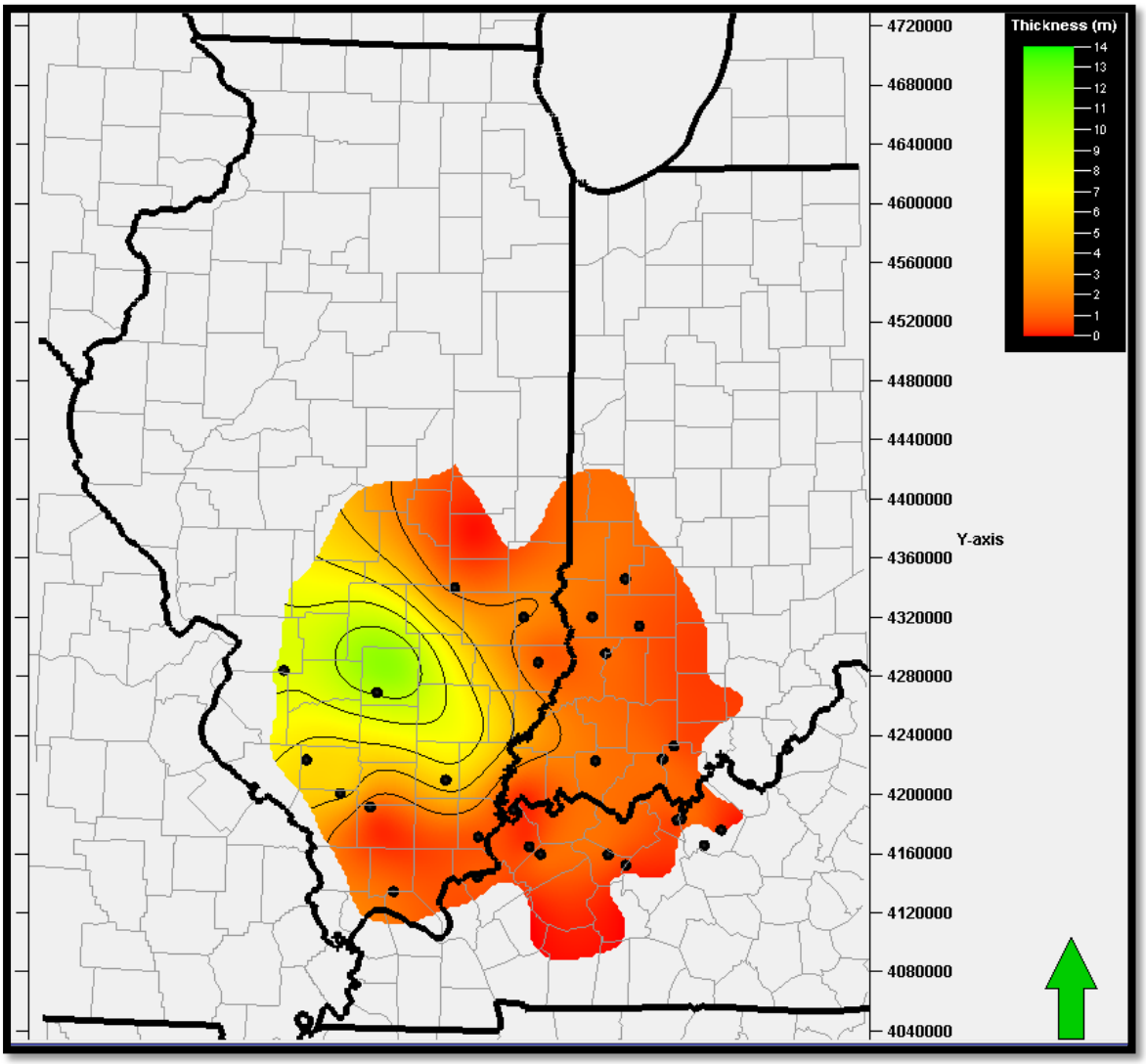

Figure 29. Net porosity grid derived from log analysis of net porosity from 32 control wells (black) with neutron porosity logs across the potential reservoir domain portion of the St. Peter Sandstone in the Illinois Basin.

A model for variation in reservoir rock sedimentary facies, petrologic, and petrophysical properties in the St. Peter Sandstone is documented in previous published studies (Barnes, and others, 1992a; Barnes and others, 1992b; Drzewiecki, and others, 1994; Girard and Barnes, 1996; Stonecipher, 2000). At least 3 distinct reservoir rock types (reservoir facies 1, 3, and 4) were recognized in 4 distinct lithofacies (1-4) in this study and in agreement with previous studies, each with variable porosity to permeability relationships having close linkage to stratigraphic position, primary depositional facies and diagenetic modification.

We reviewed stratigraphic, sedimentologic, and petrophysical properties in core and wire-line logs in the context of these previous models to establish the distribution and characteristic porosity-permeability relationships of these distinctive reservoir rock types. The first criteria used in well log analysis of reservoir rock types was the stratigraphic distinction of "restricted marine sandstone and argillaceous dolomite (lithofacies 1 and 2, non-reservoir, Figure 8 and 9) of the lower St Peter Sandstone from "open marine" shelf sandstone facies (lithofacies 3 and 4, Figure 8 and 9) in the upper St. Peter.

Sedimentary lithofacies, petrographic and petrologic analysis, including special core analysis studies were used to characterize and quantify reservoir properties in these 3 reservoir rock types (reservoir facies {r-f} 1, 3, and 4). The large core analysis and wire-line log data set available at the Michigan Geological Repository for Research and Education (MGRRE) at Western Michigan University, Kalamazoo, MI, provided the opportunity to validate and establish well log criteria for the discrimination of these distinct reservoir rock types reliably identified in conventional core. Discrimination of distinct reservoir rock types from modern well logs from the St. Peter Sandstone, through core to well log calibration/correlation, and the application of appropriate porosity cutoff values, by facies, to well log and net porosity analysis are intended to reduce uncertainty and increase precision in SRE.

The "Lower" St. Peter Sandstone; Reservoir Facies 1

Lithofacies 1 is typically very well sorted, fine- to medium-grained, quartz sandstone with abundant current induced sedimentary structures including cross-bedding and planar laminations and planar-tabular to tangential cross-bed sets, although stylolitic alteration of primary sedimentary structures typically obscures textural details. Ubiquitous, very well rounded quartz sand grains are consistent with aeolian processes in the source area of the Wisconsin highlands and the Canadian Shield the north-west and north-east (respectively) surrounding the Michigan basin (Dott, and others, 1986; Stonecipher,

2000). Bioturbation is uncommon, but locally intense. Scour surfaces and intraformational dolomicrite rip-up clasts are also common and suggest frequent subaerial exposure and early lithification in a clastics dominated but carbonate prone, peritidal setting.

Barnes and others (1992a) report interbedded fine-grained, laminated and less common, thicker bedded silty to argillaceous dolomicrite with minor shale, siltstone, and anhydrite with the cross-bedded quartz sandstone lithofacies 1 throughout the lower part of the St. Peter Sandstone in Michigan referred to as lithofacies 2. These lithofacies typically comprise the lower 50-75% of the St. Peter Sandstone (Figure 8 and 9) although basinal facies changes influence the distribution of these rock types. Significant increase in the proportion of argillaceous dolomicrite occurs toward the south and east in the basin and is attributed to increased distance from the probable clastic source terrain to the north and west (Barnes, and others, 1992a). These authors interpret these lithofacies of the "lower" St. Peter as a broad complex of tidally influenced sand flats, tidal channels, and upper shoreface depositional environments and associated lagoons in the central Michigan basin. These facies are generally not present in the upper Mississippi Valley outcrop area and were probably deposited prior to transgressive inundation of adjacent arch areas.

Most strata in the "lower" St. Peter have very low porosity due to pervasive quartz overgrowth cementation and/or pressure solution (see photomicrograph for scenario A, Figure 34). Spatially and stratigraphically limited intervals of good reservoir quality in r-f 1 are present in many wells, however as a result of variation in diagenetic alteration related to the presence of early carbonate cement and subsequent cement dissolution (Stonecipher, 2000).

The stratigraphic distribution of lithofacies 1 (r-f 1) in the lower St. Peter is identified by PEF curve values < 2.5 barns/electron and gamma ray log response below 20 API units in association with high gamma ray log response due to argillaceous dolomitic strata of lithofacies 2 (Figure 30a; non-reservoir, below the green line STPR_B1, Figure 9-12). K-feldspar silt is abundant and contributes to the high gamma ray log signal of this portion of the St. Peter. Figure 30 is a representative display of modern well log response along with conventional core porosity versus permeability semi-log plot from r-f 1 from a well in west-central Lower Michigan, permit number 40556. This display shows the relationship amongst log response, lithofacies, reservoir facies and cut-off porosity values derived from an exponential permeability to porosity transform equation for r-f 1. The effective porosity cutoff value is 7.6%ϕ in this well with r^2 (correlation coefficient) of 0.84. A compilation of similar analysis for each of the 3 reservoir facies is shown in Figure 36.

The "Upper" St. Peter Sandstone; Reservoir Facies 3 and 4

A detailed study of core and log data from the "upper" St. Peter Sandstone was conducted in the course of this work by Zdan (2013). In many parts of the Michigan Basin, the upper St. Peter consists of 2 lithofacies (lithofacies 3 and 4) with distinct reservoir properties (r-f 3 and 4). These strata comprises a transgressive, fining upward grain-size trend interpreted as the transition from shoreface to offshore transition to more distal carbonate depositional environments in the Glenwood Formation above (Barnes et al., 1992a, 1996; Zdan, 2013; Figures 9, 19a and b).

Lithofacies 4 is burrowed quartzo-feldspathic sandstone. This moderate to poorly sorted, coarse- to fine-grained, dolomitic and argillaceous sandstone is transitional upwards from lithofacies 3 (Figure 31a) and, where present, always represents the uppermost section of the St. Peter Sandstone. Lithoacies 3 is a tan to off-white, moderate to bimodally sorted, fine- to coarse grained quartz sandstone with gamma ray log response typically below 20 API units. Gamma ray log (GR) response is the primary criteria for distinguishing lithofacies 3 from lithofacies 4 in un-cored wells. In wells containing the "upper" St. Peter, facies 4 displays a steadily increasing GR response punctuated by frequent GR spikes, resulting in a "saw-tooth" pattern with broad troughs (Figure 31a and b). The curve's broad troughs reflect the burrowed quartzo-feldspathic sandstone of lithoacies 4, while the GR spikes represent inferred marine drowning surfaces observed in core. GR troughs alone (ignoring the GR peaks) display an overall increasing GR response from 21 API at the contact with the top of lithoacies 3, to between 45 and 55 API at the contact with the base of the Glenwood Formation where the GR increases sharply above 150 API. The PEF curve, where below ~2.5 barns/electron, is the main criteria for identification of the top St. Peter Sandstone (Figure 8). The steady upwards increase in GR indicative of lithofacies 4 results from increasing levels of both K-feldspar and authigenic clay (Zdan, 2013). This relationship is supported by scatter plots of K-feldspar and clay content (from petrographic point count) versus GR log response and framework grain mineralogy (Figures 32a and b).

An important petrologic distinction between r-f 3 versus 4 is substantially greater intergranular cement and intergranular clay in r-f 4 (Figure 33) in association with increased detrital k-feldspar (Figure 32b). Zdan (2013) verified previous petrologic models for diagenesis in the "upper" St. Peter (Barnes and others, 1992a; 1992b; Girard and Barnes, 1996; Barnes, 2010) and presented an updated model for paragenesis of quartz, carbonate, and clay cements in these reservoir strata (Figure 34). Microporosity associated with intergranular authigenic clay cement, and related to primary detrital framework grain k-feldspar content, typically decreases permeability relative to porosity compared to uncemented

sandstone that is more common in quartzose sandstone of r-f 3. Example displays of modern well log response and conventional core porosity versus permeability semi-log plots (Figures 35a and b) show the relationship amongst lithofacies, reservoir facies and cut-off porosity values derived from an exponential permeability to porosity transform equation for r-f 3 and 4. Figure 36 is a compilation of porosity cutoff values by well for each r-f present in that well and statistical treatment to establish log porosity cutoff values for net porosity evaluation for 3 reservoir facies; 1, 3, and 4 in the St. Peter Sandstone in Michigan.

Stratigraphic thickness, sedimentary depositional lithofacies, and depth of burial control reservoir quality in the St. Peter Sandstone in the Michigan basin. A structural cross section (Figure 37 right, see stratigraphic cross section, left, for section location map, in red on the inset overburden map) from south (left) to north (right) in western Lower Michigan from the St. Peter Sandstone pinch-out in the south (no storage capacity) to increased thickness in the St. Peter at relatively shallow burial depth to the north (best reservoir quality & good storage capacity), and finally to thick but deeply buried St. Peter furthest north with little reservoir quality/storage capacity due to extensive, depth of burial induced quartz overgrowth cementation. Note that the Mount Simon sandstone is a highly prospective sequestration target in southwestern Lower Michigan (southern-most log) while not prospective to the north, at greater burial depth, where the St. Peter Sandstone has substantial storage potential. Stratigraphic cross section (left) for the same wells shows porosity logs with a 10% cutoff (red fill) and resultant net porosity in red at the bottom of each log display.

Special Core Analysis of St. Peter Sandstone Reservoir Facies in Michigan

Special core analysis, including mercury injection capillary pressure (MICP), relative permeability, and CT scan measurements, was undertaken on representative samples of reservoir facies in the St. Peter Sandstone from conventional core samples. MICP results are presented here.

MICP Analysis – St. Peter Sandstone Reservoir Facies 1

Results still to be determined.

MICP Analysis – St. Peter Sandstone Reservoir Facies 3 and 4

Several samples from r-f 3 and 4 were analyzed using a micrometrics porosimeter at the Ohio State University, SEMCAL analytical lab. Figure 38a and b is a plot and table showing pore geometry characteristics. On the MICP plot, pore throat radius (right vertical scale) and generalized pore size classification (left vertical scale) versus mercury saturation/percentage of pore volume are shown. Reservoir facies 3 is dominated by mega-pore throats with better flow properties compared to r-f 4,

which is dominated by macro- to micro-pore throats. An excellent reservoir quality sample from the Mount Simon in Michigan is also shown for comparison. These results are interpreted to represent the generally good reservoir quality in r-f 3 and the detrimental effect of intergranular clay cements on reservoir quality in r-f 4 producing reservoir rock with generally small throated pores, good porosity but poor permeability.

SRE for the St. Peter Sandstone in Michigan using Enhanced Reservoir Characterization Techniques

SRE methodology described by Goodman and others (2011) incorporates a range of storage efficiency factors to accommodate the uncertainty related to input parameters for the calculation of total bulk volume of pore space and displacement efficiency in GCS saline reservoirs (see SRE FOR THE ST. PETER SANDSTONE IN THE MICHIGAN AND ILLINOI BASINS**,** above). The SRE methodology discussed here incorporates enhanced reservoir characterization and results in enhanced precision for SRE through the elimination of uncertainty related to total bulk volume of pore space and the application of efficiency factors related to displacement efficiency, only.

Net porosity values were calculated using the average of the neutron porosity and density porosity curves in modern well logs from 252 control wells (Figure 39a-c). The log analysis criteria for discrimination of r-f 1, 3 and 4 were applied as screens for each distinct reservoir facies in the logs and individual net porosity values by facies were calculated for each control well. The values of net porosity for each reservoir facies in each control well were then gridded into 1 km cells to generate a total bulk volume of pore space grid for each facies (Figures 39a-c). A final total bulk volume grid was also generated by using the sum of net porosity from all 3 reservoir facies in each control well (Figure 40).

The total net porosity grids were then used as input to the SRE expression along with constant ρ = 0.7 and storage efficiency factors (for clastics and reflecting displacement efficiency only) of P_{10} = 7.4%, P_{50} = 14%, and P_{90} = 24% (Goodman and others, 2011). **Final SRE for the St. Peter Sandstone in Michigan is P_{10} = 15.4 Gt, P_{50} = 29.2 Gt, and P_{90} = 50.1 Gt**.

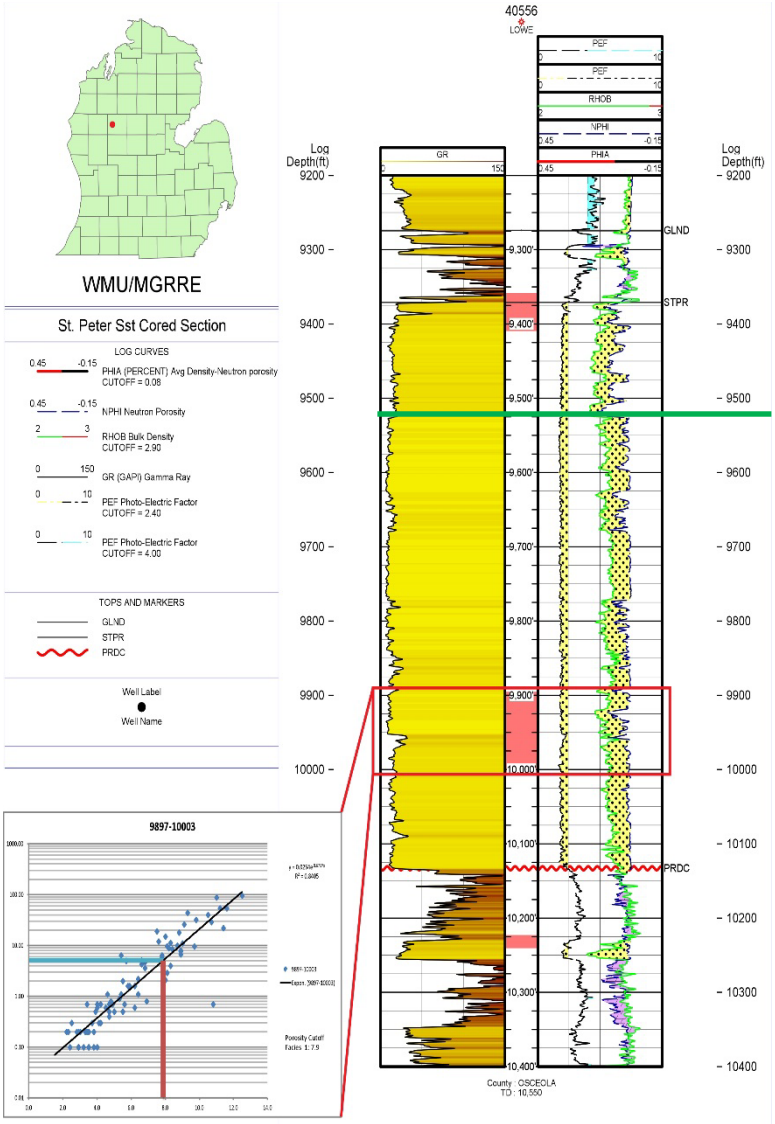

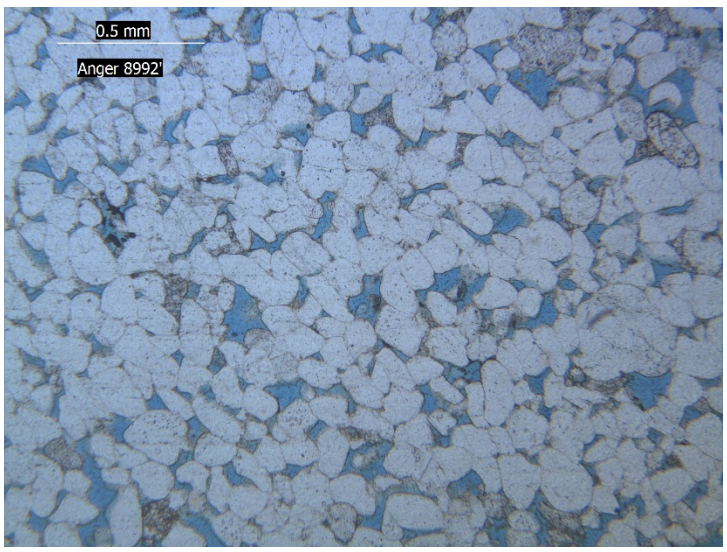

Figure 30a. . Modern log display from the St. Peter Sandstone showing the location of conventional core r-f 1 and semi-log porosity versus permeability plots of conventional core data. The exponential transform equation (black line) is used to determine a cutoff porosity value related to 5 md permeability (representing a conservative estimate of effective permeability) for r-f 1 as defined by log criteria. Correlation coefficients for other wells are not always so well correlated.

Figure 30b (below left). Photomicrograph of a typical reservoir rock in r-f 1.

Figure 30c (below right). Conventional core section of a typical reservoir rock in r-f 1

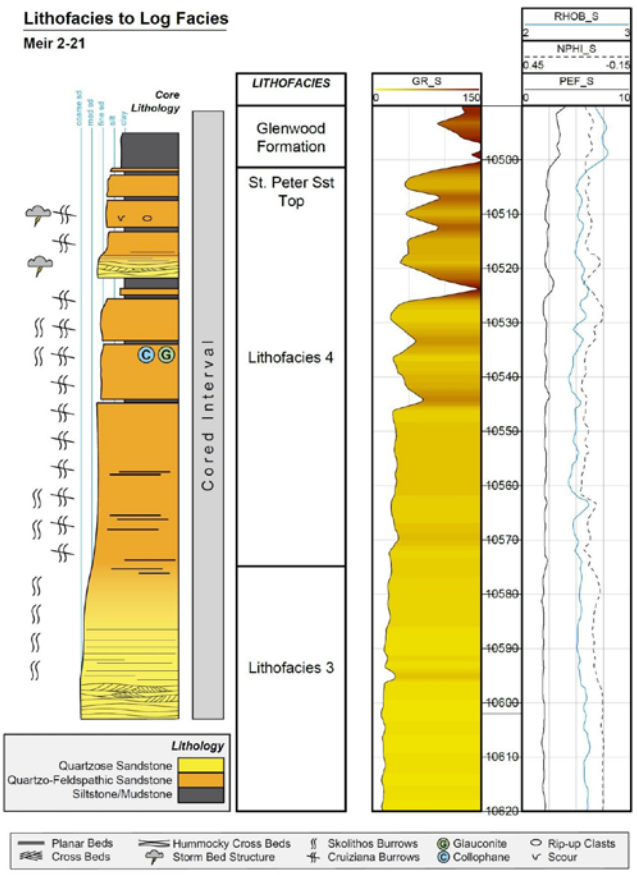

Figure 31a (left). Core to wireline log correlations. Displayed are lithofacies and corresponding wireline log responses at Meir 2-21, Ogemaw County. Note increasing gamma ray up-section, From Zdan, 2013.

Figure 31b (below). Stratigraphic cross section showing facies correlation between Hunt Martin 1-15 (Gladwin County) reference well for previous work and Meir 2-21 and Trout 3-18 (Ogemaw County to the north and east) reference well, from Zdan (2013).

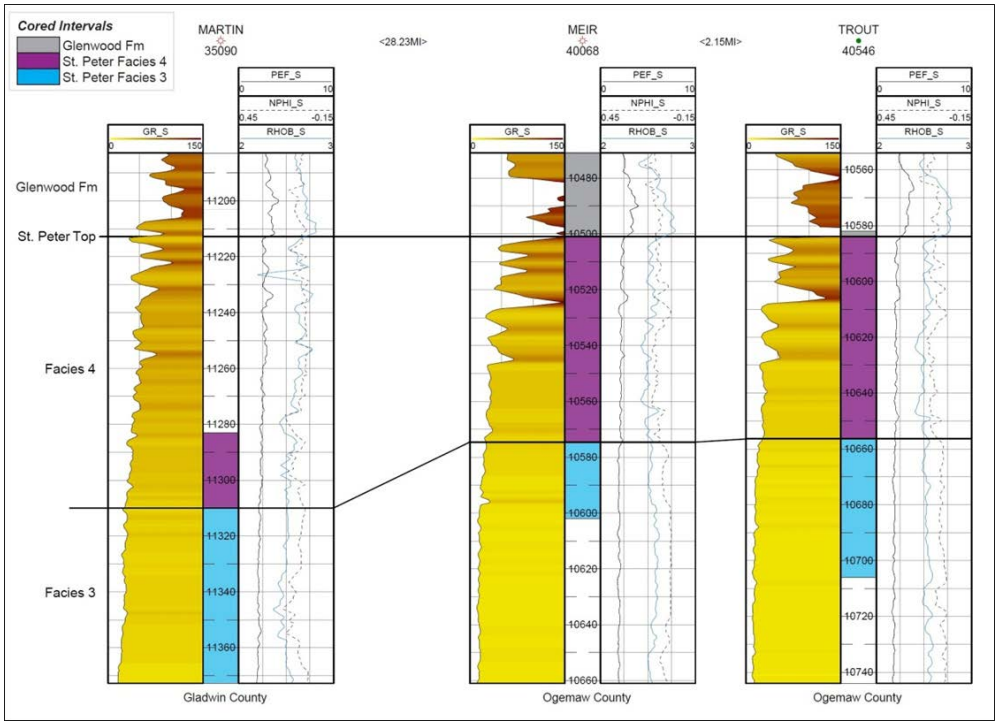

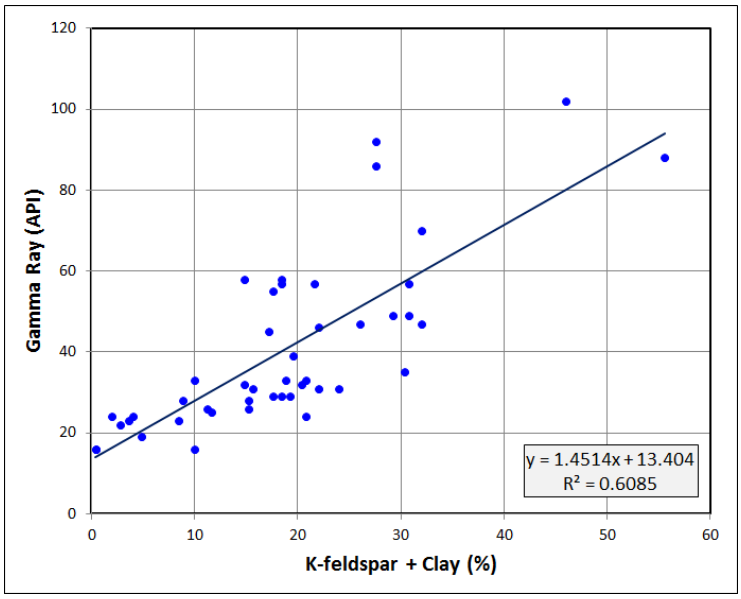

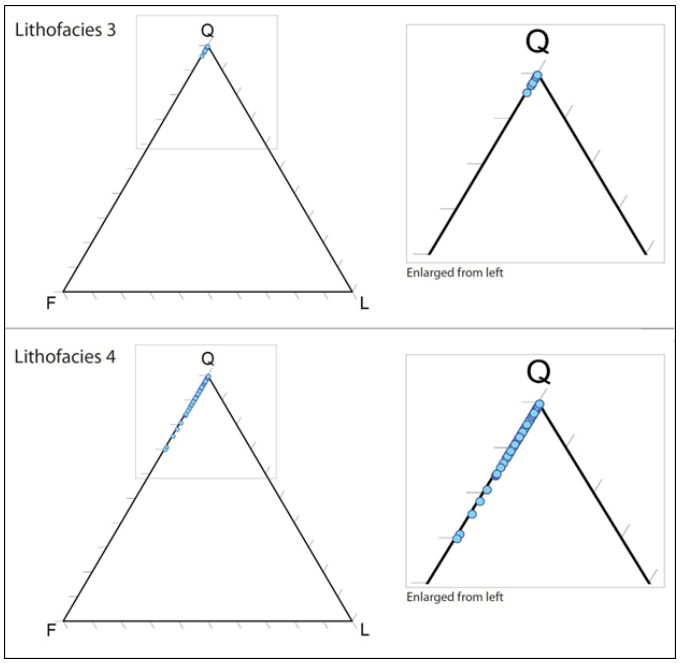

Figure 32a (left). Gamma ray verses combined K-feldspar and clay (%) for Meir 2-21, 10501'-10602' MD, with trend line, demonstrating the relationship between K^{40} isotope composition and mineralogy.

Figure 32b (right). Detrital quartz, K-feldspar, lithic fragment (QFL) plots for facies 3 and facies 4. Note nearly pure quartz detrital composition in facies 3, while K-feldspar content in facies 4 may be as high as 30%. No lithic fragments were counted in either facies.

	Facies	Qtz	K-Feld	Dolo	Qtz-Og	Clay	Glauc	Collo	Pore	Cment total	Detrital	Minus Cement Porosity
Average	4	73.0	4.6	3.8	2.5	11.6	-	-	4.5	17.9	78.0	22.4
Stdv	4	8.1	4.8	8.1	4.4	7.9	-	-	4.7	8.1	8.0	8.0
Median	4	73.2	3.2	0.8	0.0	12.4	-	-	3.2	16.8	78.8	21.2
Average	3	84.8	0.9	0.0	4.5	5.4	-	-	4.4	9.9	86.0	14.3
Stdv	3	3.2	0.8	0.0	4.8	5.2	-	-	2.6	3.8	3.5	3.5
Median	3	84.6	0.2	0.0	3.6	3.8	-	-	4.2	9.4	85.0	15.0

Figure 33. Table showing the distribution of intergranular authigenic clay in reservoir facies versus 3 from petrographic point count (Zdan, 2013). Reservoir facie 3 has substantially less intergranular cement and intergranular clay.

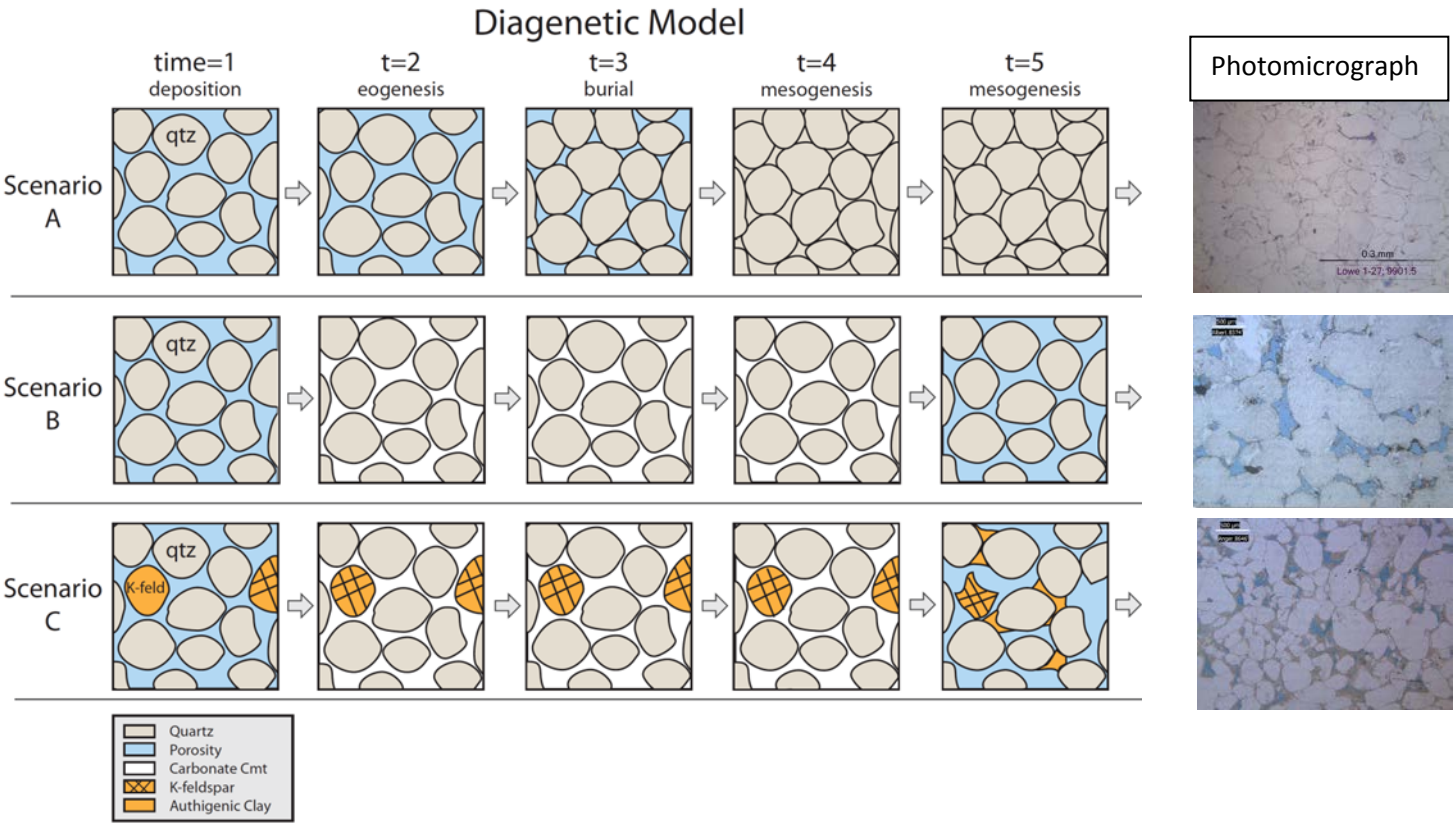

Figure 34. Petrographic model showing 3 diagenetic pathway scenarios A, B, and C, and photomicrographs of examples. In scenario A, quartzose sandstone (lithofacies 1 & 3; r-f 1 & 3) is subject to relatively rapid burial, little early (eogenetic) cementation, compaction, and extensive development of mesogenetic quartz overgrowth cement and pressure solution occluding all effective porosity. In scenario B, quartzose sandstone (lithofacies 1 & 3; r-f 1 & 3) experiences prolonged subaqueous exposure at the sea floor, develops early marine cement, and late dissolution porosity, maintaining high minus cement porosity. In scenario C, upper offshore feldspathic sandstone (lithofacies 4; r-f 4) experiences the same depositional and eogenetic conditions as scenario B. Additionally, detrital feldspar grains dissolve providing K^+ for local precipitation of pore-lining, authigenic clay (Zdan, 2013).

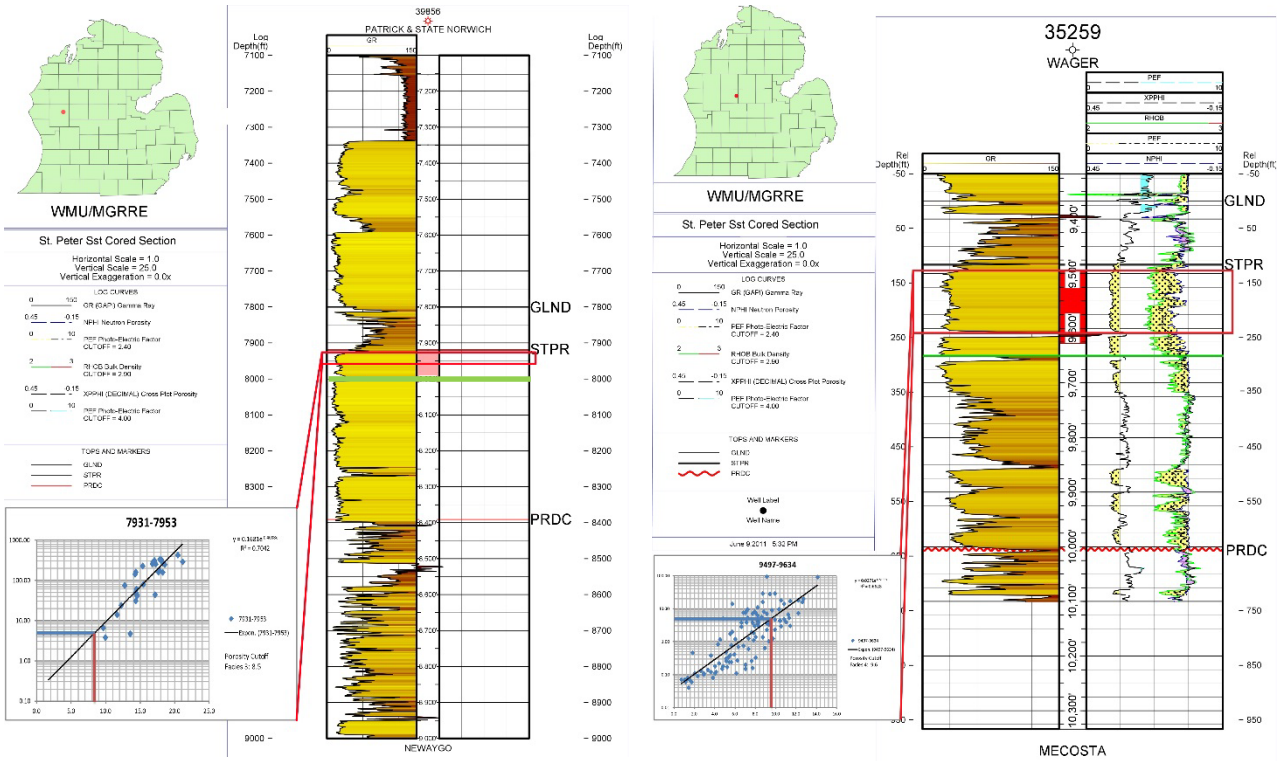

a. b.

Figure 35a and b. Modern log displays from the upper St. Peter Sandstone showing the location of conventional core r-f 3 (35a, left), and r-f 4 (35b, right) and semi-log porosity versus permeability plots of conventional core data for each these reservoir facies. The exponential transform equation (black line) is used to determine a cutoff porosity value related to 5 md permeability (representing a conservative estimate of effective permeability) for each reservoir facies as defined by log criteria. Exponential correlation coefficients from other wells shown in Figure 4 have considerable range.

Porosity cutoff from transform using core analysis(Ø & K) cross plots at 5 md permeability				
Core Name	**Well Permit #**	**Facies 1**	**Facies 3**	**Facies 4**
Anger	41137		10	
Anger	41137	8.8		
Blair	34292		9	10.3
State Garfield	43570			11.4
State Garfield	43570			10.9
Gernaat	35781		8.4	
Harter	42596	6.9		
Hunt-Martin	35090	6	7	11.2
Lowe	40556	7.9		10.2
Patrick	39856		8.8	11
Robinson	35482		9	9.9
State Summerfield	42156			9.8
State Foster	42396	7.6		
State Garfield	45446	8.1		
Sundmacher	39433			13.6
Wager	35259			9.6
Avg. Porosity Cutoff by r-f:		**7.6%ϕ**	**8.7%ϕ**	**10.8%ϕ**
Std. Deviation		0.98	0.99	1.17
Min		6	7	9.6
Max		8.8	10	13.6

Figure 36. Summary of porosity cutoff values, by facies, as derived from core analysis data

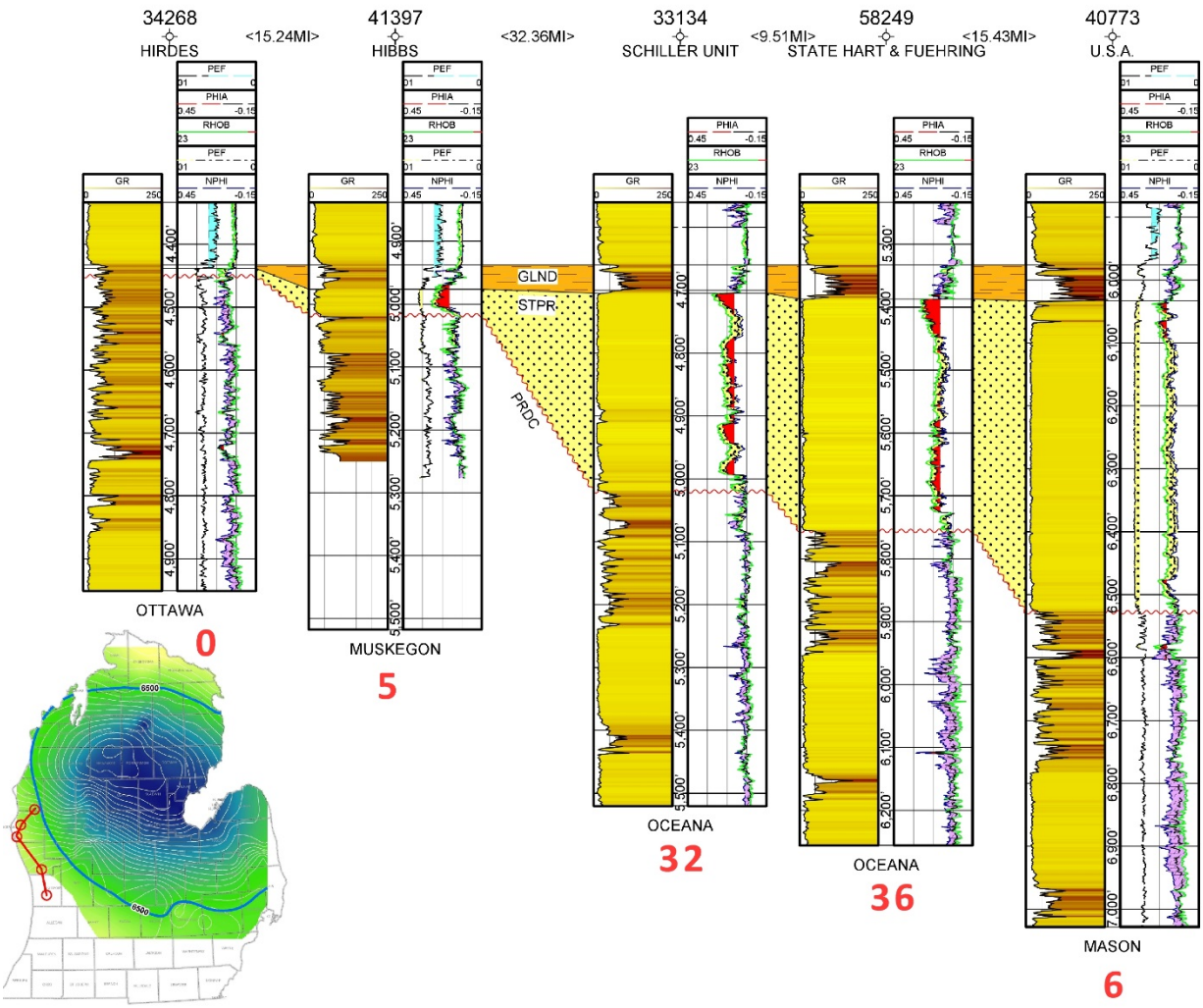

Figure 37a. Stratigraphic cross section showing stratigraphic pinchout of the St. Peter Sandstone to the south, thickening of the formation towards the basin center and distribution of reservoir quality. Red shading on the porosity logs indicates >10%ρ

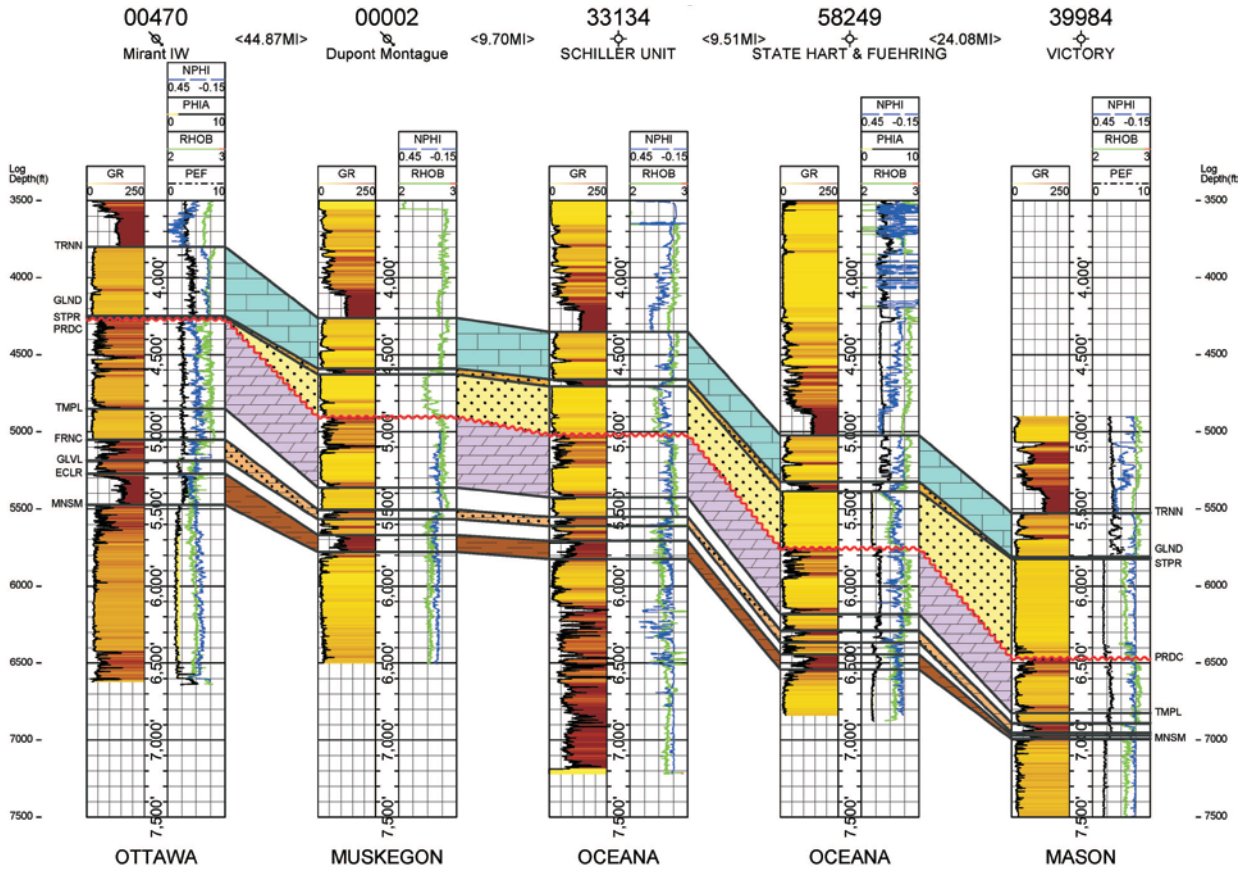

Figure 37b. Structural cross section in westrn Lower Michigan showing the burial depth relationship to reservoir quality. See text for discussion.

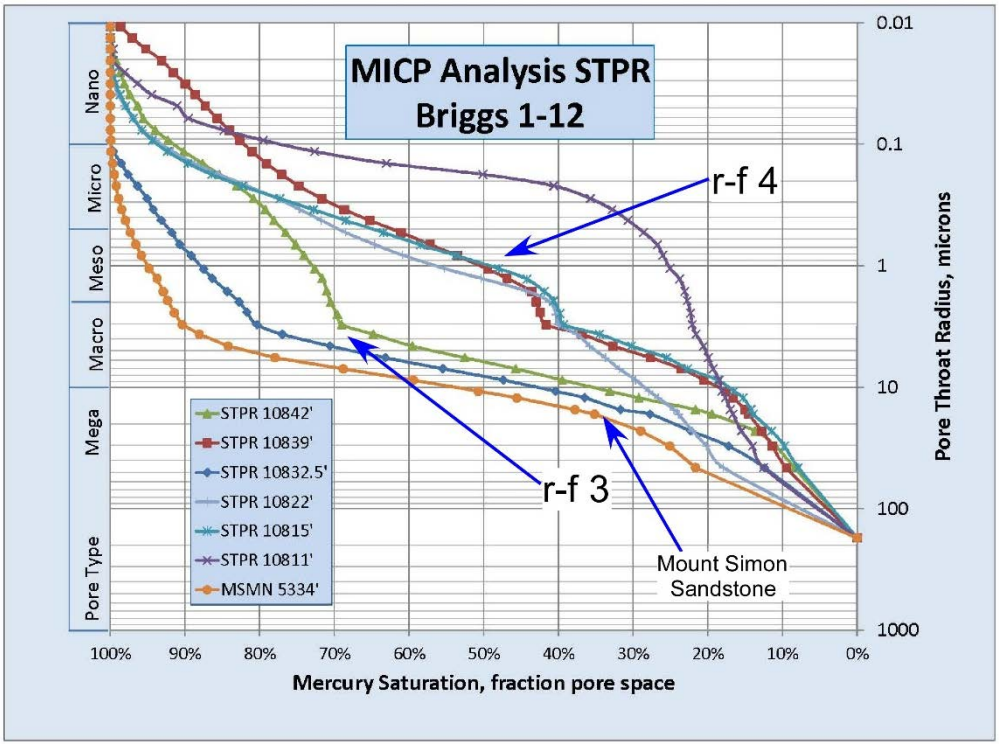

Briggs 1-12 Sample #	*Sample*	*Ø*	*Perm*	*Median pore throat radius (µm)*	*r^{35} (µm)*	*Pore Type*
	MSMN 5334	12.1	54.1	10.2	16.7	Mega
1	STPR 10832.5	9.6	30.1	8	12.5	Mega
2	STPR 10842	8.6	30.6	6	10.5	Mega
3	STPR 10822	11	23.1	1.3	5.5	Macro
4	STPR 10839	3.5	2.5	1.1	4.1	Macro
5	STPR 10815	6.2	26.2	1	3.5	Macro
1	STPR 10811	2.8	21 (?)	0.18	0.3	Micro

Figure 38 (above). MICP plot of pore throat size versus mercury saturation/fraction of pore space for representative samples of r-f 3 and 4 in the St. Peter Sandstone. Figure 38 (below). Table showing convention core analysis results (porosity and permeability), median pore throat radius, r^{35} the dominant pore throat radius for non-wetting fluid phase flow, and generalized pore size characteristics. See text for discussion.

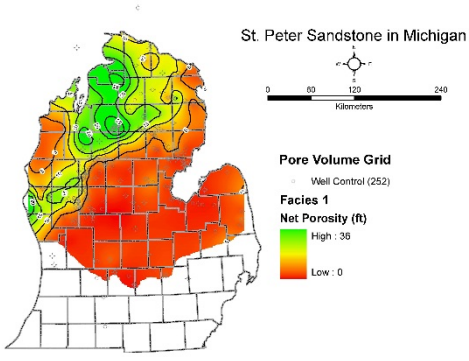

a.

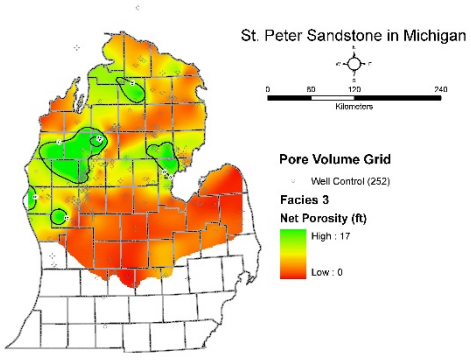

b.

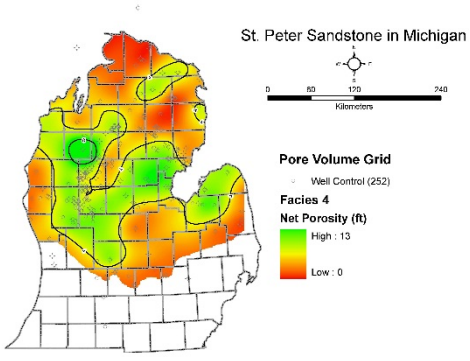

c.

Figure 39, b, and c. Total pore volume grids calculated from net porosity for each reservoir facies determined from advanced reservoir characterization in modern well logs from the St. Peter Sandstone.

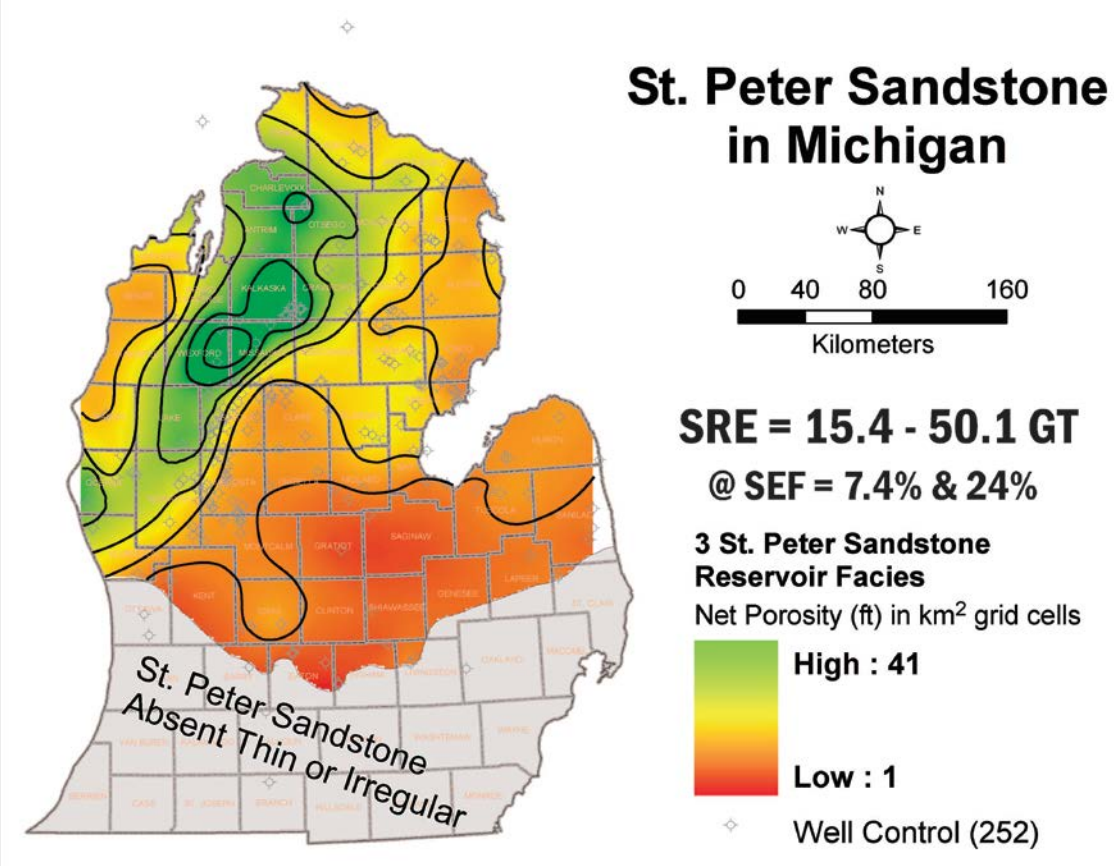

Figure 40. Total SRE for the St. Peter Sandstone (composite of 3 reservoir facies).

CONCLUSIONS

A summary of the results from the four different approaches to SREs is provided in two different tables for the basins analyzed (Figures 41 and 42). Recent work by Ellett and others (2013) and Barnes and others (2013) suggests that the application of the standard storage efficiency factors published in the DOE methodology (Goodman and others, 2011) to a reservoir volume that has been spatially constrained based on water quality (10,000 ppm TDS requirement) or CO_2 phase criteria (>800 m depth for suitable P and T conditions) will effectively underestimate the resource. This underestimation occurs because the SEFs use a range of 0.2 to 0.8 in the net-to-total area term, however, the net area of the potential reservoir volume has already been explicitly defined and reduced from the total area as a result of honoring the above criteria. Applying the published SEFs effectively over-discounts the resource because of the inclusion of this net-to-total area term in the total SEF for saline formations. Permitting of CO_2 injection into saline formations by the EPA UIC program requires that storage is only considered for the portion of the formation in which total dissolved solids of native brines exceed 10,000 ppm. Furthermore, to ensure that CO_2 remains in a dense supercritical phase, the standard approach to defining the net area of a potential saline formation storage reservoir is to remove any area of the storage formation that has a reservoir/seal contact boundary lying above 800 meters depth as we've done in this study. Thus it should be noted that the SREs calculated by means of the first two methods in this study (i.e., using gross thickness and either average porosity or a depth-dependent porosity model) are considered to be conservative estimates.

Additionally, we note that applying the SEFs from the DOE methodology to our results for methods 3 (net porosity calculation) and 4 (advanced reservoir characterization, Michigan Basin only) effectively overestimates SRE since the SEF values assume that the geologic terms are known exactly (i.e., equal to 1) and uncertainty is accounted for only in the displacement terms. In reality there still exists some uncertainty in the geologic terms even though we have reduced the effective pore volume by our net porosity analysis. Thus for the SREs calculated by methods 3 and 4 (i.e., using net thickness and advanced reservoir characterization) the results should be considered to be somewhat optimistic estimates.

Method	Method Description	MI CO2 Storage Capacity P10 Estimate (Gt)	MI CO2 Storage Capacity P50 Estimate (Gt)	MI CO2 Storage Capacity P90 Estimate (Gt)	Total Pore Volume (MI) in km^3
Method 1	**Gross Isopach, constant porosity (6.7%), constant CO2 density (.737 ton/m3), ξ = 0.51 & 5.4% (from CO2 Atlas III for clastics)**	**3.3**	**13.0**	**35.1**	**881.2**
Method 2	**Gross Isopach, depth dependent porosity, constant CO2 density (.737 ton/m^3), ξ = 0.51 & 5.5% (from CO2 Atlas III for clastics)**	**3.0**	**11.7**	**31.6**	**793.0**
Method 3	**Net Porosity methodology (1 STPR cutoff value), constant CO_2 density (.737 ton/m3), ξ = 7.4% & 24% (from CO2 Atlas III for clastics)**	**10.7**	**20.2**	**34.7**	**196.0**
Method 4	**Net Porosity methodology (3 STPR facies in MI), constant density (.737 ton/m3), ξ = 7.4% & 24% (from CO2 Atlas III for clastics)**	**15.4**	**29.2**	**50.1**	**283.2**

Figure 41. SRE summary for methodologies or approaches described in this paper for the Michigan Basin. ξ symbol represents storage efficiency factor.

Storage Resource Estimate Approach	CO2 Storage Resource (billion metric tons) P10 estimate	P50 estimate	P90 estimate	Total pore volume km^3
Approach 1: Gross thickness; mean porosity of 14.1%; constant CO2 density of 0.7 g/cc; E factors of 0.51% (P10), 2.0% (P50) and 5.4% (P90).	1.0	4.1	11.0	291.6
Approach 2: Gross thickness; depth-dependent porosity model; constant CO2 density of 0.7 g/cc; E factors of 0.51% (P10), 2.0% (P50) and 5.4% (P90).	0.6	2.3	6.1	161.2
Approach 3: Net porosity calculation; constant CO2 density of 0.7 g/cc; E factors of 7.4% (P10), 14.0% (P50) and 24.0% (P90).	11.2	21.2	36.4	216.7

Figure 42. Same as table in figure 41 except SRE summary is for the Illinois Basin analysis of the St Peter Sandstone.

REFERENCES

Barnes, D. A., Lundgren, C. E., and Longman, M. W., 1992a, Sedimentology and Diagenesis of the St. Peter Sandstone, Central Michigan Basin, United States: American Association of Petroleum Geologists Bulletin, v. 76, no. 10, pp. 1507-1532.

Barnes, D.A., Girard, J.P. & Aronson, J.L., 1992b. KIAr Dating of Illite Diagenesis in the Middle Ordovician St Peter Sandstone, Central Michigan Basin, USA: Implications for Thermal History. Spec. Pubis Soc. Econ. Paleont. Mineral. 47, pp. 35-48.

Barnes, D.A., Harrison, W.B. III, and Shaw, T.H., 1996. Lower-Middle Ordovician lithofacies and interregional correlation, Michigan basin, U.S.A Geological Society of America Special Papers, 1996, 306, p. 35-54,

Barnes, D. A., 2010, Stratigraphic Controls on Diagenesis and Reservoir Quality in a Saline Reservoir Geological Carbon Sequestration Target: the Middle Ordovician St. Peter Sandstone, Michigan Basin, USA. AAPG Search and Discovery Article #90116©2010 AAPG Eastern Section Meeting, Kalamazoo, Michigan, 25-29 September 2010.

Barnes, D.A., Ellett, K.M., Sosulski, J., Rupp, J.A., and Leetaru, H., 2013, A Comparison of Geological CO_2 Storage Resource Calculation Methodologies to Evaluate Parameter Sensitivity and Reduce Uncertainty: Case study of the St. Peter Sandstone (Ordovician) in the Illinois and Michigan Basins: AAPG S&D Article #80278.

Buschbach, T.C. and Bond, D.C., 1974, Underground Storage of Natural Gas in Illinois-1973. State of Illinois Department of Registration and Education, Illinois State Geological Survey, Illinois Petroleum 101, 80 pp.

Catacosinos, P. A. and P. A. Daniels, Jr., 1991, Stratigraphy of Middle Proterozoic to Middle Ordovician Formations of the Michigan Basin, in Catacosinos, P.A. and Daniels, P.A., eds., Early Sedimentary Evolution of the Michigan Basin, GSA Special Paper 256, P. 53-71.

Dapples, E, C, 1955, General lithofacies relationship of St. Peter Sandstone and Simpson Group: AAPG Bulletin, v, 39, no, 4, p, 444-467,DOE-NETL, 2012, Carbon Utilization and Storage Atlas, 130 pp.

Dott, R, H" Jr., C W, Byers, G, W, Fielder, S, R, Stenzel, and K. E, Winfree, 1986, Aeolian to marine transition in Cambro-Ordovician cratonic sheet sandstones of the northern Mississippi Valley, U.S.A.: Sedimentology, v, 33, p, 345-367.

Droste, J. P., Abdulkareem, T. F., and Patton, J. B., 1982, Stratigraphy of the Ancell and Black River Groups (Ordovician) in Indiana. Indiana Geological Survey Occasional Paper 36, 15 pp.

Drzewiecki, P. E., Simo, J. A., Brown, P. E., Castrogiovanni, E., Nadon, G. C., Sheppard, L., Valley, J.W., Vandrey, M. R., Winter, B., and Barnes, D., 1994. Diagenesis, Diagenetic Banding, and Porosity evolution of Middle Ordovician St. Peter Sandstone and Glenwood Formations in the Michigan Basin. In: P. Ortoleva (ed.) Basin Compartments and Seals, Am. Assoc. Petrol Geol. Mem. 61, 179-199.

Ellett, K., Zhang, Q., Medina, C., Rupp, J., Wang, G., and Carr, T., 2013, Uncertainty in regional-scale evaluation of CO_2 geologic storage resources—comparison of the Illinois Basin (USA) and the Ordos Basin (China): Energy Procedia, v 37, 5151-5159, doi:10.1016/j.egypro.2013.06.430.

Girard, J-P and Barnes, D A, 1995, Illitization and Paleothermal Regimes in the Middle Ordovician St. Peter Sandstone, Central Michigan Basin, United States: K-Ar, Oxygen Isotope, and Fluid Inclusion Data. Am. Assoc. Pet. Geology Bull., v. 79, p.49-69.

Goodman, A., Hakala, A., Bromhal, G., Deel, D., Rodosta, T., Frailey, S., Small, M., Allen, D., Romanov, V., Fazio, J., Huerta, N., McIntyre, D., Kutchko, B., Guthrie, G., 2011. U.S. DOE methodology for the development of geologic storage potential for carbon dioxide at the national and regional scale. International Journal of Greenhouse Gas Control 5, 952–965.

Hoholick, J.D., Metarko, T., and Potter, P.E., 1984, Regional variations of porosity and cement: St. Peter and Mount Simon Sandstones in Illinois Basin: American Association of Petroleum Geologists Bulletin, v. 68, p. 733–764.

Kolata, D. R., 1991. Tippecanoe I Sequesnce overview: Middle Ordovician Series through Late Devonian Series, in Leighton, M. W., Kolata, D. R., Oltz, D. F., and Eidel, J. J. (eds), Interior Cratonic Basins, American Association of Petroleum Geologists Memoir 51, 87-99.

Leetaru, H. E., Brown, A. L., Lee, D. W., Senel, O., and Couëslan, M. L., 2012, CO2 injectivity, storage capacity, plume size, and reservoir and seal integrity of the Ordovician St. Peter Sandstone and the Cambrian Potosi Formation in the Illinois Basin: DOE report number DOE/FE0002068-1.

Mai, H" and R, H, Dott, Jr., 1985, A subsurface study of the St. Peter Sandstone in southern and eastern Wisconsin: Wisconsin Geological and Natural History Survey 47, 26 p.

Medina, C.R., Rupp, J.A., and Barnes, D.A., 2011, Effects of reduction in porosity and permeability with depth on storage capacity and injectivity in deep saline aquifers: A case study from the Mount Simon Sandstone aquifer, International Journal of Greenhouse Gas Control, Volume 5, Issue 1, January 2011, Pages 146-156

NETL, 2012. US Carbon Utilization and Storage Atlas, 4th edition (Atlas IV): US Department of Energy, National Energy Technology Laboratory.

Owen, D. D., 1847, Preliminary report of the geological survey of Wisconsin and Iowa: U. S. General Land Office Rept., p. 170.

Pitman, J. K., Goldhaber, M. B., and Spoetl, C., 1997. Regional Diagenetic Patterns in the St. Peter Sandstone: Implications for Brine Migration in the Illinois Basin, US Geological Survey Bulletin 2094-A, 17 pp.

Stonecipher, S. A., 2000, Cautions about using Core Analysis Data: The St. Peter Sandstone, Michigan Basin, in Applied Sandstone Diagenesis- Practical Petrographic Solutions for a Variety of Common Exploration, Development, and Production Problems, SEPM Short Course No. 50.

Udegbunam, E. 0., Huff, B. G., Kemppainen, C., and Morgan, J., 2001, Integrated Geological and Engineering Study and Reservoir Simulation of the St. Peter Sandstone Gas Storage Reservoir at the Hillsboro Field, Montgomery County, Illinois. Illinois Petroleum 156,

USGS, 1992, GROUND WATER ATLAS of the UNITED STATES: Iowa, Michigan, Minnesota, Wisconsin, HA 730-J, Olcott, P.J.

USGS, 1995, GROUND WATER ATLAS of the UNITED STATES: Illinois, Indiana, Kentucky, Ohio, Tennessee, HA 730-K, Orville B. Lloyd, Jr., and William L. Lyke

Willman, H. B., Atherton, E., Buschbach, T. C., Collinson, C., Frye, J. C., Hopkins, M. E., Lineback, J. A., and Simon, J. A., 1975, Handbook of Illinois stratigraphy: Illinois State Geological Survey Bulletin 95, 261 p.

Zdan, Stephen A., 2013, Stratigraphic Controls on Diagenetic Pathways in the St. Peter Sandstone, Michigan Basin. Unpublished MSc thesis, Western Michigan University, 2013.